Self-reinforced polymeric materials: A review
Kmetty A., Barany T., Karger-Kocsis J.

Self-Reinforced Polymeric Materials: A Review

Ákos KMETTY[1], Tamás BÁRÁNY[1*], József KARGER- KOCSIS[1,2]

1- Department of Polymer Engineering, Budapest University of Technology and Economics,

   H-1111 Budapest, Műegyetem rkp. 3., Hungary

2- Polymer Technology, Faculty of Engineering and Built Environment, Tshwane University of Technology, Pretoria 0001, Republic of South Africa

   * Author to whom correspondence should be addressed,

   E-mail: barany@eik.bme.hu

Abstract

The preparation, properties and applications of self-reinforced polymeric materials (SRPMs), representing an emerging family of composite materials, have been surveyed. SRPMs were classified according to their constituents (single- and multi-component), production (in one-step /in situ/ or in multi-step procedures /ex situ/) and spatial alignment of the reinforcing phase within the matrix (in one-, two- or three-dimensions; 1D, 2D and 3D, respectively). The pros and cons of the related processes and products were introduced and further development aspects with SRPMs highlighted. It was pinpointed that the recycling (i.e. reprocessing via remelting) and the possibility to produce lightweight structures are the driving forces of SRPMs' development.

Key words: polymers, self-reinforced, processing, microstructure, structure-property relationships, semicrystalline polymers, application

Table of contents

Nomenclature				
$a_{c,n}$	[kJ/m^2]	impact strength (notched)	MD	machine direction
$a_{c,n,L}$	[kJ/m^2]	longitudinal impact strength	MFC	microfibrillar composite
$a_{c,n,T}$	[kJ/m^2]	transversal impact strength	OPIM	oscillating packing injection molding
D	[mm]	extruder screw diameter	PA	polyamide
E_B	[GPa]	E-modulus (flexural)	PA-12	polyamide-12
E_t	[GPa]	E-modulus (tensile)	PA-6.6	poliamid-6.6
$E_{t,L}$	[GPa]	E-modulus (tensile, longitudinal)	PBA	polybutyl acrylate
$E_{t,T}$	[GPa]	E-modulus (tensile, transversal)	PCTG	polycyclohexane-terephthalate glycol
k	[W/mK]	thermal conductivity	PE	polyethylene
L	[mm]	extruder screw length	PEEK	polyether-ether-ketone
p	[MPa]	processing pressure	PEN	polyethylene-naphthalate
p_A	[MPa]	pressure amplitude	PET	polyethylene-terephthalate
T_D	[^{o}C]	drawing (stretching) temperature	PETG	polyethylene-tereptalate glycol
T_g	[^{o}C]	glass transition temperature	PMMA	polymethyl-methacrylate
T_{proc}	[^{o}C]	processing temperature	POM	polyoxymethylene or polyacetal
$T_{proc,opt}$	[^{o}C]	optimal processing temperature	PP	polypropylene
T_m	[^{o}C]	melting temperature	PPS	polyphenylene-sulfide
T_{melt}	[^{o}C]	melt temperature	PS	polystyrene
T_{mold}	[^{o}C]	mold temperature	PTFE	polytetrafluoro-ethylene
v	[mm/min]	extrusion velocity	PVC	polyvinyl-chloride
λ	[-]	drawing ratio	PVDF	polyvinylidene-fluoride
σ_B	[MPa]	tensile strength	rPP	random polypropylene copolymer
$\sigma_{B,L}$	[MPa]	longitudinal tensile strength	SCORIM	shear-controlled orientation injection molding
$\sigma_{B,T}$	[MPa]	transversal tensile strength	SEM	scanning electron microscopy
σ_F	[MPa]	flexural strength	SRPM	self-reinforced polymeric material
σ_Y	[MPa]	yield strength	SRPP	self-reinforced polypropylene
BP	[MPa]	based pressure for VIM	TD	transverse (to machine) direction
CBT		cyclic butylene terephthalate oligomer	TEM	transmission electron microscopy
CM		conventional injection molding	TMA	thermo mechanical analysis
CNF		carbon nanofiber	UD	unidirectional alignment, structure
CP		cross-ply structure	UHMPE	ultra high modulus polyethylene
DMA		dynamical mechanical analysis	UHMWPE	ultra high molecular weight polyethylene
DSC		differential scanning calorimetry	VF [Hz]	vibration frequency
EP		ethylene-propylene copolymer	VIM	vibration injection molding
EPR		ethylene-propylene rubber	VPA [MPa]	vibration pressure amplitude
GF		glass fiber	α-PP	isotactic PP (alpha form)
HDPE		high density polyethylene	α-rPP	random polypropylene copolymer (alpha form)
hPP		polypropylene homopolymer	β-PP	isotactic PP (beta form)
iPP		isotatic polypropylene		
LCP		liquid crystalline polyester		

1. Introduction

Nowadays considerable research activities, accompanied with commercial interest, are devoted to all-polymeric materials, and especially to self-reinforced versions. In all-polymeric materials both the reinforcing and matrix phases are given by suitable polymers. In self-reinforced polymeric materials (SRPM) the same polymer forms both the reinforcing and matrix phases. SRPMs are also referred to single-phase or homocomposites. Moreover, in the open literature also such polymer composites are termed to SRPMs in which the reinforcement and matrix polymers are different but belong to the same family of polymers (see later).

SRPMs may compete with traditional composites in various application fields based on their favorite performance/cost balance. With respect to their performance the easy recycling has to be emphasized. Note that SRPM represents likely the best recycling option when reprocessing via remelting is targeted. Accordingly, SRPMs can be considered as environmentally benign materials. The concepts used to produce SRPMs can be adapted also to biodegradable polymers to improve their property profile whereby even their degradation properties can be tailored upon request.

A further driving force of SRPMs is the possibility to manufacture lightweight parts and structures because the density of the SRPMs is well below those of traditional ones. The latter contain namely reinforcements, like glass (density: 2.5-2.9 gcm^{-3}), carbon (density: 1.7-1.9 gcm^{-3}), basalt (density: 2.7-3.0 gcm^{-3}), aramid (density: 1.38-1.44 gcm^{-3}), and/or fillers like talc (density: 2.7-2.8 gcm^{-3}), chalk (density: 1.1-2.5 gcm^{-3}), silica(density: 2.1-2.6 gcm^{-3}) and thus the density of the corresponding composite is usually higher than that of SRPM.

The basic concept of self-reinforcement is to create a one-, two- or three-dimensional alignment (1D, 2D and 3D, respectively) within the matrix by suitable manners which fulfils the role of matrix reinforcement. Reinforcing action requires that the structure generated possesses higher stiffness and strength than the matrix, and in addition, it is well "bonded" to the matrix polymer. As a consequence the stress can be transferred from the "weak" matrix to the "strong" reinforcing structure which is the "working principle" of all composites. The reinforcing structure can be produced during one (in situ) or more processing steps (ex situ). This along with the spatial alignment of the reinforcement may serve for their straightforward classification. The latter is disclosed in Figure 1 which serves further on as guide-line in this article to survey SRPMs.

From historical point of view the development of SRPMs started with the in situ production of 1D-reinforced variants. This occurred mostly with solid phase extrusion forming, and techniques exploiting melt shearing in the solidifying melts. The related

operations resulted in 1D aligned supermolecular structures (whereby indirectly the covalent bond strength of the macromolecules utilized) acting as reinforcement in SRPMs. The term "supermolecular structure" already suggests that SRPMs are almost exclusively semicrystalline polymer-based systems. The reinforcing structure in them has either different crystalline and/or supermolecular (also referred to higher order structure) structures or it is given by a preform, prefabricate (e.g. fiber, tape and their different textile architectures) with higher (and different) crystallinity compared to the matrix. 1D reinforcement can also be generated by multi-step stretching. The related technology, practiced for example in fiber spinning operations, is grouped into multi-step (ex situ) production of single-component SRPMs (cf. Figure 1). According to our terminology self-reinforced polypropylene (PP) composites, produced only from fibers or fabrics as preforms, are classified as multi-step products of single-component SRPMs which may exhibit 1D (unidirectional fiber alignment), 2D (fabric plies) or 3D (e.g. braided structure) reinforcements. In other words, when an SRPM is produced solely from preforms, prefabricates instead of primary granules of a given polymer, it is classified as a product of multi-step processing.

Commercial break-through with SRPMs occurred recently. Self-reinforced PP composites (also called all-PP composites) are now available on the market under the trade names Curv®, Pure®, Armordon®. Curv® is a single-component multi-step product usually with 2D (fabric) reinforcement, whereas Pure® and Armordon® is a two-component multi-step version originally with 1D reinforcement (being a stretched tape having different PP grades in its core and surface layers).

As mentioned before, the majority of SRPMs is based on semicrystalline polymers. On the other hand, amorphous matrix based SRPMs can also be created when interpreting the "self-reinforcement" in a broader sense, i.e. extending it for a given family of polymers. For example, amorphous copolyesters can be reinforced by polyethylene-terephthalate (PET) fibers whereby keeping the melt reprocessability. It is noteworthy that transesterification reactions in the melt (which can be triggered by additional additives) guarantee the necessary adhesion between the reinforcing PET and amorphous copolyester matrix. In other SRPM versions the difference in the melt temperature of semicrystalline polymers, belonging to the same family, is exploited. One can find reports on such all-PA or self-reinforced PA materials the constituents of which are different PAs, for example the matrix is given by PA-12 of low melting temperature, whereas the reinforcement is from a higher melting PA, such as PA-6 or PA-6.6.

2. Self-Reinforced Polymeric Materials

In this chapter the grouping, as outlined in Figure 1, will be followed. Accordingly, the single- and multi-component SRPMs will be treated separately by considering their production (i.e. in situ or ex situ) and spatial reinforcing structure (i.e. 1D, 2D or 3D).
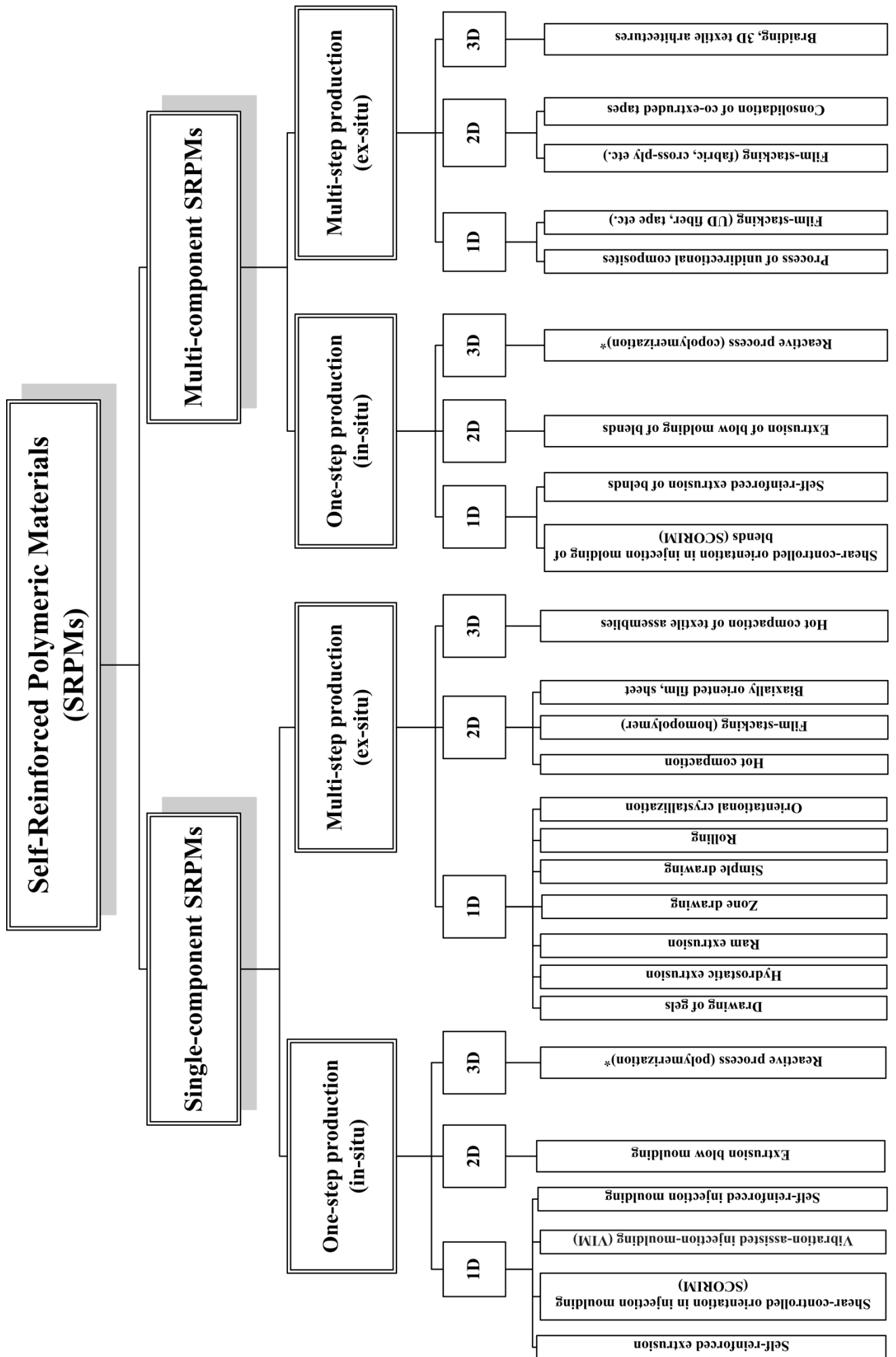
Self-Reinforced Polymeric Materials (SRPMs)

- **Single-component SRPMs**
  - **One-step production (in-situ)**
    - **1D:**
      - Self-reinforced extrusion
      - Shear-controlled orientation in injection moulding (SCORIM)
      - Vibration-assisted injection-moulding (VIM)
      - Self-reinforced injection moulding
    - **2D:**
      - Extrusion blow moulding
    - **3D:**
      - Reactive process (polymerization)*
  - **Multi-step production (ex-situ)**
    - **1D:**
      - Drawing of gels
      - Hydrostatic extrusion
      - Ram extrusion
      - Zone drawing
      - Simple drawing
      - Rolling
      - Orientational crystallization
    - **2D:**
      - Hot compaction
      - Film-stacking (homopolymer)
      - Biaxially oriented film, sheet
    - **3D:**
      - Hot compaction of textile assemblies

- **Multi-component SRPMs**
  - **One-step production (in-situ)**
    - **1D:**
      - Shear-controlled orientation in injection molding of blends (SCORIM)
      - Self-reinforced extrusion of blends
    - **2D:**
      - Extrusion of blow molding of blends
    - **3D:**
      - Reactive process (copolymerization)*
  - **Multi-step production (ex-situ)**
    - **1D:**
      - Process of unidirectional composites
      - Film-stacking (UD fiber, tape etc.)
    - **2D:**
      - Film-stacking (fabric, cross-ply etc.)
      - Consolidation of co-extruded tapes
    - **3D:**
      - Braiding, 3D textile architectures

Figure 1 Classification of self-reinforced polymeric materials (SRPMs), *not yet explored

2.1 Single-Component SRPMs

2.1.1 One-step (in situ) production

1D self-reinforcing structure can be produced by extrusion molding whereby the extruder is equipped with die having a convergent section (cf. Figure 2). The convergent section (with an angle of 45° or higher) is foreseen to generate the molecular orientation via extensional flow that is "frozen" in the subsequent sections of the die (calibration zone). Pornimit and Ehrenstein [1] used this technique to manufacture self-reinforced HDPE. It was shown that the oriented molecules act as (self) row nuclei and trigger the formation of a cylindritic and shish-kebab-type supermolecular structures (Figure 2). As control parameter of the formation of the self-reinforcement the temperature program of the die (affecting the pressure build-up within) was identified. Cooling the outcoming zone of the die a high extrusion pressure could be reached which supported the formation of the shish-kebab crystals. The self-reinforced HDPE rod exhibited considerably higher stiffness, strength and highly reduced thermal shrinkage when measured in the reinforcing direction.
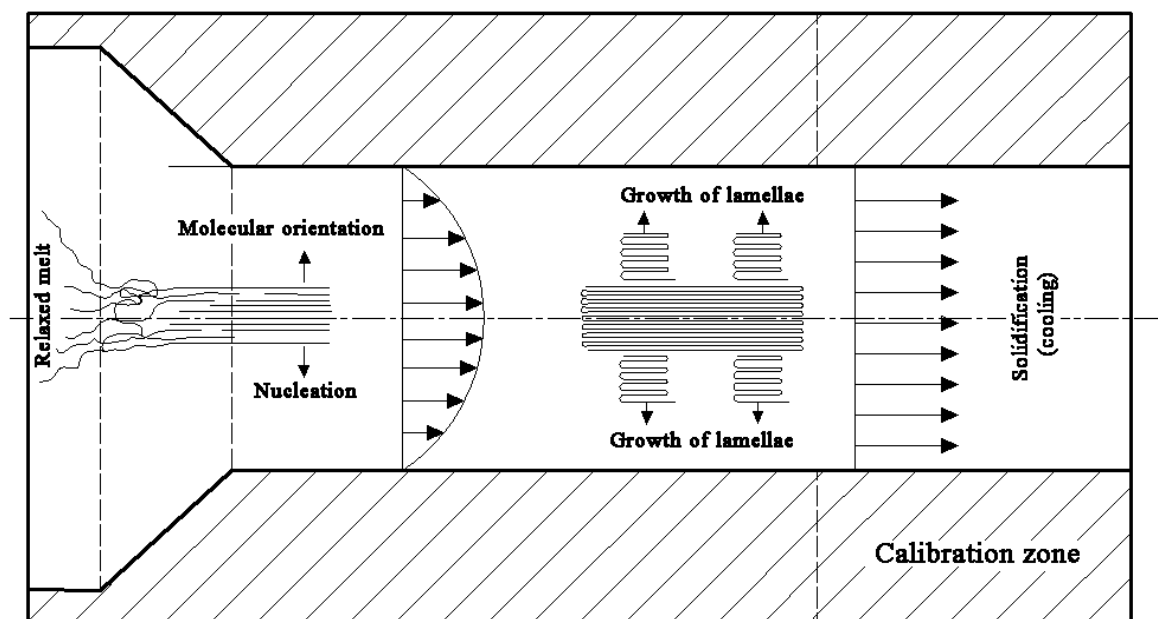
Figure 2: Scheme of the 1D supermolecular structure formation in a die with a convergent section during extrusion molding

Although the shish-kebab structure is known from the mid 1960s, the mechanism of its formation is still debated. Kornfield et al. [2] in their recent work proposed that long chains are not the dominant species of the shish formation as thought before. Nevertheless, the presence of long macromolecules strongly favors the propagation of shish.

The basic prerequisites of the extrusion procedure yielding 1D self-reinforcement were identified as follow [3]: molecular orientation in the melt via forced extensional flow, processing close to the crystallization temperature of the polymer, and "fixing" of the

resulting structure in the final section of the die by rising the pressure. DSC investigations showed that the melting peak of the self-reinforced HDPE was shifted towards higher temperatures (by ca. 4$^{\mathbf{o}}$C). The thermal stability of the oriented crystals could be well detected by polarized optical microscopy during which different fusion temperatures were set prior to the subsequent crystallization steps.

Farah et al. [4] developed shear-induced crystallization layers in iPP via a slit die attached to a twin-screw extruder. The output rate was below 10 kg/h. The die temperatures were set between 169 and 230$^{\mathbf{o}}$C. Rheological studies revealed that the induction time, at a given crystallization temperature, decreased as the shear rate increased. At a given shear rate the higher was the crystallization temperature, the longer the induction time was. It was observed that at given output rate, the thickness of the shear-induced crystalline layer decreased with the increase of die temperature. Three layers were found by SEM and TEM. Two layers were spherulitic while one layer was composed of highly oriented lamellae.

Huang et al. [5, 6] produced self-reinforced HDPE by using a convergent die (angle 60$^{\mathbf{o}}$) and an extrusion pressure ranging from 30 to 60 MPa. Similar to the methods in [7] the authors cooled the melt before leaving the die to 128$^{\mathbf{o}}$C. The strength of the resulting 1.5 mm thick sheets was eight times higher than that of the conventionally extruded sheet. The anisotropy in the sheets was detected in mechanical, tribological tests and demonstrated also by microhardness results.

Parallel to the works on PEs, PP was also discovered as suitable candidate for SRPM [8, 9]. Song et al. [10] produced self-reinforced PP by a conventional single-screw extruder with pressure regulation (L/D=30, maximum pressure: 100 MPa), equipped with a convergent die (entrance angle 45$^{\mathbf{o}}$) with two or more calibration (cooling) sections. The properties of the extrudate were superior to counterparts produced by the conventional extrusion molding.

Self-reinforced structure can also be generated by injection molding. The related techniques differ from one another whether the oriented structure is created outside or within the mold. Ehrenstein et al. [11] produced self reinforced material using the technique of converging die injection molding. They injected the low temperature melt into the cavity just after the melt passed a convergent die section. Note that this concept requires a careful mold construction and well defined processing conditions to avoid relaxation phenomena reducing the molecular orientation.

Those injection molding techniques which generate the self-reinforcement in the mold became far more popular than the above mentioned variant. They are known under shear-controlled orientation in injection molding (SCORIM)) [12, 13], or oscillating packing injection molding (OPIM). The common characteristic of these techniques is that the molecular orientation is set in the mold by shearing/oscillation of the solidifying melt via a suitable arrangement of pistons. The pistons start to work when the cavity is already filled.

The related mold construction may be very different [14], however in SCORIM three basic operation modes exist (cf. Figure 3).
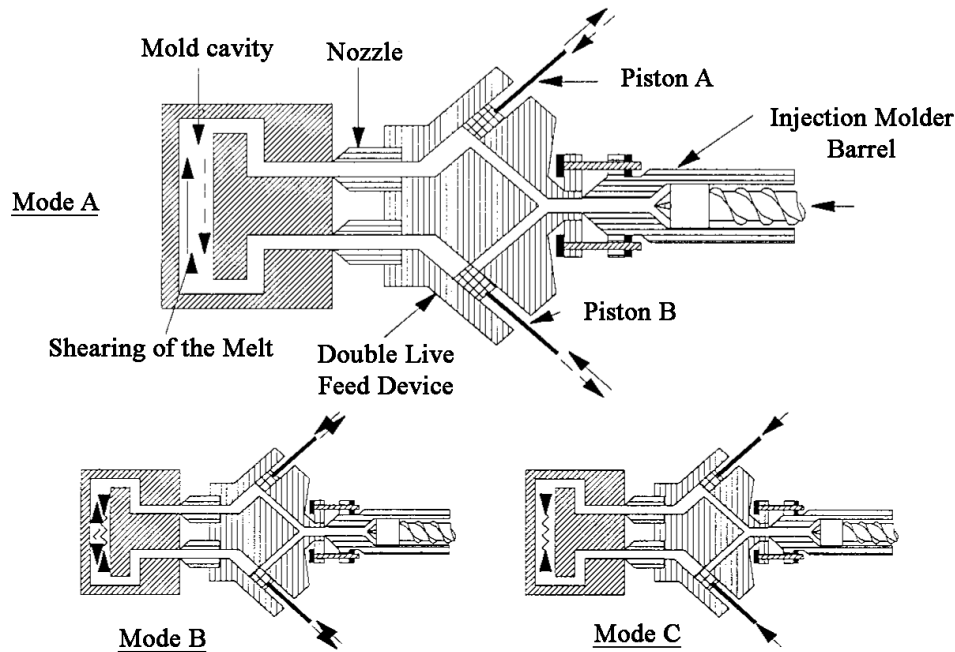

Figure 3: Scheme of the function of the SCORIM procedure [15] along with the three basic operations (A, B, and C) – Mode A: the pistons are activated 180⁰ out of phase; Mode B: pistons are activated in phase; Mode C: the pistons are held down a constant pressure.

Guan and coworkers [16] used the OPIM to produce self-reinforced HDPE. The injection pressure of ca. 41 MPa was superimposed by an oscillating packing pressure (varied between 32 and 48 MPa) with frequency of 0.3 Hz. As operation mode "A" in Figure 3 was chosen and for the temperature of the melt and mold 220 and 42⁰C were set. The molded parts were subjected to mechanical and morphological tests. The stiffness and strength of the OPIM moldings were superior to the conventional ones. Morphological studies revealed the presence of a microfibrillar structure. TEM study showed that the microfibrillar structure is composed of shish-kebab formations. Based on DSC measurements the authors concluded that the microspherulitic structure melts at 132⁰C, whereas the shish-kebab crystals at 137⁰C. In a follow-up work Guan et al. [17] adapted the OPIM on PP. Studying the effects of processing conditions the authors concluded that the mechanical properties of the moldings strongly depend on the operation mode, and on lesser extent, on the oscillation frequency, frequency/mode and frequency/time combinations.

Chen and coworkers [18] produced biaxial self-reinforced (i.e. 2D) PP by OPIM. As operation mode "A" in Figure 3 was selected and for the temperature of the melt and mold

195 and the range of 20-80⁰C, respectively, were chosen. The products exhibited quite balanced (i.e. less anisotropy) static mechanical (strength improvements compared to conventional injection molding in melt flow direction and transverse to it 55-70 and 40%, respectively), but further on a pronounced anisotropy in respect to impact strength (improvement to conventional molding in melt flow direction and transverse to it 400 and 30-40%, respectively).

Kalay et al. [15, 19] investigated the influence of PP types on the corresponding SCORIM products and deduced the basic rules on how to prepare products with optimum properties. It is the right place to emphasize that the basic advantage of SCORIM/OPIM is the pronounced orientation of the molecules in the whole cross-section of the molded parts. This is because of the repeated shearing/oscillation movements in the melt which are acting until the melt solidifies. This suppresses the relaxation of the oriented molecules.

A further variant of the injection molding resulting in self-reinforcement is the vibration injection molding (VIM), that was pioneered by Li and coworkers [20]. The working principle of VIM is depicted in Figure 4. The ram itself is a part of both the injection and vibration systems. Without vibration the set-up works as conventional injection molding (CM) unit. However, working in VIM mode, pulsations occur in the injection and holding pressure stages. This causes an effective compression and decompression of the melt and shearing at the melt–solid interface. Note that solidification is progressing from the surface to the core of the molding in the cavity. For this VIM device the main processing parameters are: vibration frequency (VF) and vibration pressure amplitude (VPA).
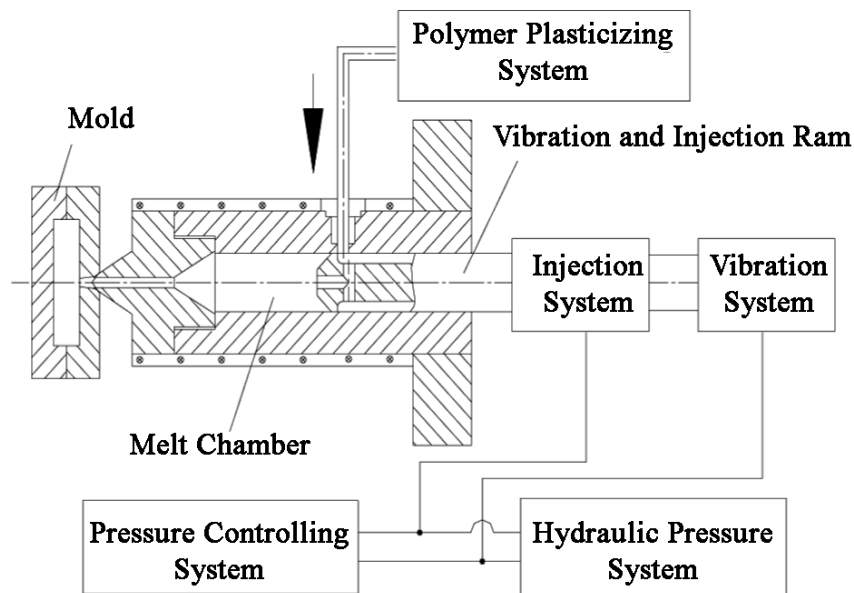

Figure 4: Working principle of the vibration injection molding [20]. "Reprinted from Polymer-Plastics Technology and Engineering, 47, Li Y. B., Chen J., Shen K. Z.: Self-reinforced isotactic polypropylene prepared by melt vibration injection molding., 47, 673-677., Copyright (2010), with permission from Taylor & Francis"

In the cited study the authors used a single screw extruder as plastification unit. The PP melt has been vibrated for 25 sec and the cooling time was fixed at 20 sec. The injection pressure for CM and the base pressure (BP) for VIM was 49.4 MPa. In the latter case the pressure amplitude was fixed at 19.8 MPa. The mechanical properties and morphology of the specimens were determined. It was found that the mechanical properties of the VIM-produced parts were enhanced compared to conventional injection molding. The yield strength steeply rose with the vibration frequency in the range of 0-1 Hz. Afterwards, a constant value was noticed for the range 1-2.5 Hz. The tensile strength increased with increasing vibration frequency. The impact strength of PP was doubled compared to the conventional molding using VIM at 2.33 Hz. The crystalline structure of the VIM-produced PP showed the simultaneous presence of the crystalline alpha, beta- and gamma-modifications of PP. In a companion study [21] using HDPE and setting the vibration frequency at 2.33 Hz and the pressure amplitude at 19.8 MPa, the authors observed the formation of a shish-kebab along with row-nucleated crystalline lamellae. Their presence resulted in an upgrade of the mechanical properties of HDPE.

Attention should be paid to a widely practiced design method in injection molded items, to the film or 'plastic' hinge. It was early recognized that the convergent (hinge) section of the molded parts of both semicrystalline and amorphous thermoplastics has a peculiar performance: it withstands multiple bending movements. Now, this design principle is used in many products of the everyday life, especially for dispensing packages. Morphological studies on such hinges [22] demonstrated the presence of strongly oriented (1 or 2D) supermolecular structures, including shish-kebab types. The hinge consisted of two highly oriented surface layers and one almost isotropic core in between. The core exhibited small-sized spherulitic structure whereas the oriented surface layers contained shish-kebab structures. The mechanical behavior of the oriented layers is similar to that of "hard elastic fibers" which show a high stiffness and a high strain recovery. So, products with film or 'plastic' hinges represent nice examples of the one-step (in situ) produced SRPCs, albeit only a given section of them is really self-reinforced.

Num.	Processing	Materials	Processing conditions	Results	Comment	Ref.
1	**Self-reinforced extrusion**	HDPE	Entrance semi-angel of 45°, p=60…100 MPa, T_{mold}=180°C	σ_B=160 MPa, E_t=2…17 GPa	Fibrillar structure (next to the die wall), Shish-kebab structure	[1]
			Entrance semi-angel of 60°, p=30…60 MPa, T_{mold}=128°C	σ_B=130...192 MPa,	Fibrillar structure, Micro hardness and light permeability are increasing	[5, 6, 23]
		PP	p=30…70 MPa, T_{mold}=160°C v=160…200 mm/min	σ_B=60 MPa, E_t=3.3 GPa	-	[10]
2	**Self-reinforced injection molding**	hPP	T_{melt}=160…190°C, T_{mold}=25…80°C,	σ_B=62…95 MPa, E_t=2…3 GPa	-	[10, 11]
3	**SCORIM /OPIM**	HDPE	T_{melt}=140…180°C, p_{proc}=25-28 MPa T_{mold}=40…60°C	$\sigma_{B,L}$=24…29 MPa, $a_{c,N,L=}$ 5…6 kJ/m^2, $\sigma_{B,T}$=25…30 MPa, $a_{c,N,T}$=5…6 kJ/m^2	Static packing	[14]
				$\sigma_{B,L}$=36…56 MPa, $a_{c,N,L}$=8…14 kJ/m^2 $\sigma_{B,T}$=23…36 MPa, $a_{c,N,T}$=2…3 kJ/m^2	Dynamic packing (f=0.2-0.5 Hz)	
			p_{proc}=32…48 MPa, T_{melt}=220°C, T_{mold}=42°C	σ_B=70…90 MPa, E_t=3…6 GPa	-	[16]
		PP	T_{mold}=42°C, T_{melt}=210-240°C,	σ_B=34…35 MPa	Static packing	[17]
				σ_B=47…53 MPa	Dynamic packing (f=0.3-1 Hz)	
		iPP	T_{mold}=20…80°C, p_{proc}=40 MPa,	$\sigma_{B,L}$=44 …55 MPa, $a_{c,N,L}$= 7…13 kJ/m^2 $\sigma_{B,T}$=35…45 MPa, $a_{c,N,T}$= 2…3 kJ/m^2	Dynamic packing f=0.125…0.5 Hz	[18]
		PP copolymer	p_{proc}=100 MPa, T_{mold}=60-110°C, T_{melt}=220…250°C,	σ_y=50…59 MPa, E_t=2…3 GPa	Different packing mode	[15, 19]
		iPP	p_{proc}=100…160 MPa, T_{mold}=60°C, T_{melt}=205…250°C	σ_y=38…77 MPa, E_t=2…3 GPa	Different packing mode	
4	**VIM**	iPP	p_{proc}=100 MPa, T_{mold}=40°C, T_{melt}=210-230°C, f= 0…2.5Hz, p_A=0..73.5 MPa	σ_y=32…38 MPa, $a_{c,n}$=11…32 kJ/m^2	-	[20]
		HDPE	p_{proc}=39.5 MPa, T_{mold}=40°C, T_{melt}=180-200°C, VF=0…2.33 Hz, p_A=0..59.4 MPa	Crystallinity=60…70%	Laminar and shish-kebab structure	[21]

Table 1: Production method, conditions and product characteristics of single-component SRPMs produced in one-step (in situ)

2.1.2 Multi-step (ex situ) production

Single-component SRPCs can also be produced by multi-step production methods, such as die- and zone-drawing, ram extrusion, hydrostatic extrusion, rolling (using various solid "preforms" which are eventually produced on-line), gel drawing or spinning (where the "preform" is a dilute polymer solution). As the reader will see in many cases the preparation of the "preform" and the generation of the reinforcing structure within occur on-line, but in different stages, steps. This is the reason why they are listed among the multi-step production methods. When the orientation, and thus creation of the reinforcing structure takes place in solid state of the polymer (i.e. below its melting temperature), the related methods are referred to solid-state processes [10].

Solid phase extrusion

The ram extrusion was developed in the early 70s. It involves the pressing of a solid preform through a metallic die of conical (convergent) shape. This technique was successfully adapted to many thermoplastics, covering not only semicrystalline (PE, PTFE, PP, PET, PA), but also amorphous versions (PS) [24]. Major problems with the ram extrusion are: very low output rate due to the very high friction between the solid polymer and die surface, and the coexistence of different morphological superstructure through the cross-section of the extrudate [25]. Legros et al. [26] studied the effects of processing conditions (additional use of lubricant, variation in the extrusion speed, use of a take-up device) of the ram extrusion on the properties of HDPE and PP rods. The experiments were performed at a barrel area/die exit area ratio of 6. The maximum draw ratio, $\lambda \sim 6$, was obtained with a low extrusion speed of 0.1 mm/s. At higher speeds, like at high extrusion temperatures, λ was markedly reduced for PP. For HDPE, the decrease in the draw ratio as a function of experimental conditions was less pronounced than for PP. Increasing draw ratio was accompanied with enhanced crystallinity, as expected. By the take-up device the relaxation phenomena in of the rod, after leaving the die, could be reduced. Note that this technique is well established for manufacturing various PTFE-based products nowadays.

By the hydrostatic extrusion [24] some drawbacks of the ram extrusion can be circumvented. For example the extrudate has a homogeneous reinforcing structure. In this process the polymer preform is pressed with the help of a hydraulic fluid through a conical die and the outcoming extrudate is pulled away – cf. Figure 5.
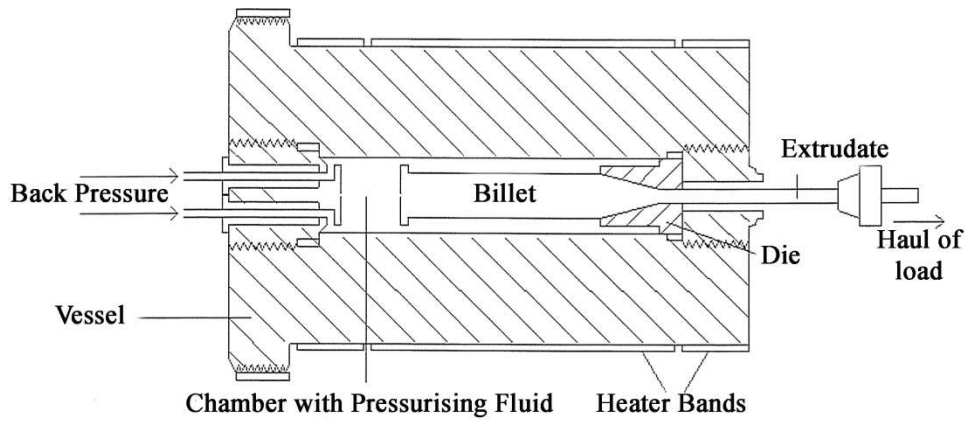
Figure 5: Working principle of the hydrostatic extrusion process schematically [24]. "Reprinted from Ward I. M., Coates P. D., Dumoulin M. M.: Solid Phase Processing of Polymers. Hanser, Munich Copyright (2010) with permission from authors"

The hydrostatic extrusion was successfully adapted to manufacture high-modulus tapes and fibers even from filled (hydroxyapatite/PE) and reinforced polymers (discontinuous glass fiber reinforced POM). Disadvantages of this process are: discontinuous operation and the very high flow stress at the exit of the die. The polymer has the highest strain rates at the exit of the conical die where the plastic strain is greatest. The strain rate sensitivity of flow stress in solid-state extrusion increases rapidly with plastic strain. The situation which incurs very high flow stresses as the polymer reaches the die exit, high extrusion pressures therefore being required [24]

The die-drawing, credited to Ward et al. [24], is a further development is this field. The change in the morphology due to die/drawing is depicted schematically in Figure 6.
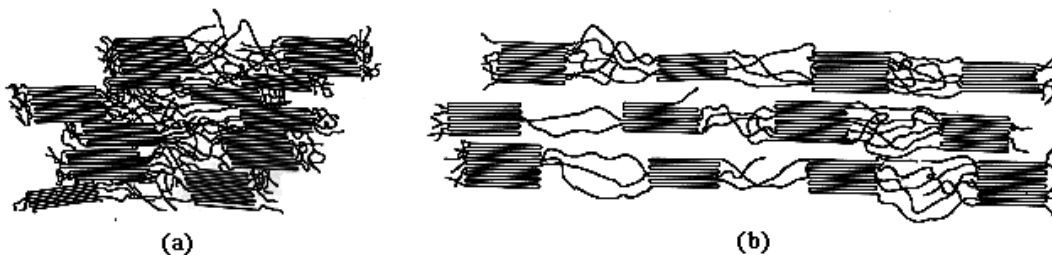
Figure 6: Morphology change due to die-drawing schematically a: unoriented phase, b: oriented phase

The advent of the die-drawing is that the draw ratio can be set accordingly. This technique was used to different polymers, like PE [27], PP [28, 29], PVC [24], PET [24], PEEK [24], PVDF [24], POM [30]. Owing to the high molecular orientation the related products exhibited pronounced improvements in the E-modulus, strength, barrier and solvent resistance. In addition, the extrudates

were less prone to creep than the conventionally produced counterparts. This method is used to produce PE (gas, water) and PVC pipes (drainage), and PET containers (food storage) [24].

Super drawing

Two-stage draw technique was applied to super-drawing of PTFE virgin powder by Endo and Kanamoto [31]. In the first-stage the compression-molded PTFE film was solid-state co-extruded (extrusion draw ratio (EDR) between 6 and 20) at 10°C below the T_m. The second-stage draw was made by applying a pin-draw technique in the temperature range covering the static T_m of PTFE. The maximum achieved total draw ratio was 160. The maximum tensile modulus and strength at 24°C reached 102 ± 5 and 1.4 ± 0.2 GPa, respectively.

Rolling

Rolling processes can induce a permanent deformation in the morphology by transforming the initial spherulitic to a fibrillar structure. It can be achieved by series of pairs of rolls (heated or not) and temperature-conditioning steps. Rolling is usually preferred for semicrystalline instead of amorphous polymers because the latter show more pronounced relaxation behavior [24, 32]. PE and PP used for room temperature rolling whereby a thickness reduction ratio of up to ~5:1 was reached. At high speeds (as high as 20 m/min) rolling occurred adiabatically. As a consequence the chemical and thermal stability of the polymer should be considered. The rolling process is increased the crystalline, and amorphous molecular orientations, and thus enhanced both the strength and E-modulus of the polymer [33].

It is well known that plastic deformation of crystalline polymers, especially on drawing, is associated with cavitation. Cavitation, however, can be suppressed by applying compressive stress during orientational drawing. This was demonstrated by Polish researchers who developed a method, called rolling with side constraints [34-37]. The materials used were mostly HDPE and PP.

Galeski [38] reviewed the structure-property relationships in isotactic PP and HDPE produced by rolling with side constraint. Rolling was done in a specially constructed apparatus at various speeds (0.5 to 4 m/min for iPP and 200 mm/min for HDPE) at different temperatures. Both E-modulus and ultimate tensile strength increased with increasing deformation ratio. The maximum strength/deformation ratio values were 340 MPa/10.4 and 188 MPa/8.3 for iPP and HDPE, respectively.

Mohanraj and coworkers [39] prepared highly oriented polyacetal (POM) bars via constrained rolling process. In this process the heated polymer billet is deformed in a channel given by the circumference of the bottom roll that provides lateral constraint to the material when it deforms.

POM was rolled below the crystalline melting temperature. The modulus and strength parallel to the rolling direction increased almost linearly with the compression ratio.

Gel drawing

Via gel drawing (spinning) films and fiber can be produced from a dilute polymer solution. This requires, however, a polymer with high mean molecular weight and suitable molecular weight distribution characteristics. The molecules are less entangled in the gel that guarantees the drawing to high degrees [40-42]. Oriented synthetic fibers of UHMWPE (Dyneema (www.dsm.com) and Spectra (www51.honeywell.com)) can be formed by gel spinning (gel drawing process) which have tensile strength as high as 2.8 GPa. These fibers are mostly used to produce ballistic vests covers, safety helmets, cut resistant gloves, bow strings, climbing ropes, fishing lines, spear lines for spear guns, high-performance sails, suspension lines in parachutes etc. (tensile strength of the ballistic materials ~ 3.5 GPa).

Orientation drawing

Elyashevich and coworkers [43, 44] prepared high-modulus and high-strength PE fibers via orientation drawing. Drawing took place between the glass transition (T_g) and melting temperature (T_m) of the given polymer. During orientation the folded chain crystal lamellae rotate, beak-up, defold and form finally aligned chain crystals (cf. Figure 7)
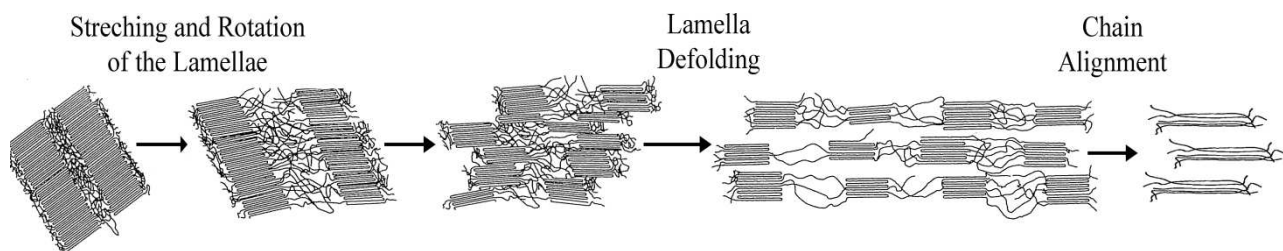

Figure 7: Scheme of chain orientation

Fibers with very high orientation (draw ratio) were produced in one or more drawing steps. In the latter case, the isothermal drawing temperature was increased from one to the next drawing step. Elyashevich et al. [43, 44] manufactured in one-step orientation PE fibers having E-modulus and tensile strength of 35 and 1.2 GPa, respectively.

Baranov and coworkers [45] produced ultra high modulus PP tapes by a two-step isothermal drawing process. The isothermal drawing of the parent film was done in a tensile testing machine, equipped

with a thermostatic chamber. The first drawing occurred at 163-164°C, while the second one at 165°C. The E-modulus and strength of the tapes were 30-35 and 1.1 GPa, respectively. PP and PET tapes, strips are widely used for packaging purpose. Their tensile strength ranges are 220-350 MPa and 430-570 MPa for PP and PET, respectively. Morawiec et al. [46] demonstrated that the strength of PET, even from scrap (recycled beverage bottles), may reach 700 MPa when suitable orientation conditions prevail. This was demonstrated using an on-line two step extrusion drawing unit.

The structural "basis" of high-strength and high-modulus polymers is well reviewed by Marikhin [47]. This chapter helps the interested reader also to trace pioneering activities of researchers in the related fields.

Alcock and coworkers [48] produced highly oriented PP tapes by extrusion and drawing steps. The tensile deformation was achieved by pulling a tape from one set of rollers at 60°C, through a hot air oven to a second set of rollers at 160-190°C. The tapes classified in two series; Series A describes PP tapes drawn to varying draw ratios at the same drawing temperatures, while Series B covered PP tapes drawn to $\lambda = 13$ at a range of drawing temperatures in the second drawing stage. The results showed that the density was approximately constant with increasing draw ratio until $\lambda = 9.3$, above which it sharply dropped. The decrease in density was associated with a change in opacity of the tape due to the onset of microvoiding within the tape. Karger-Kocsis et al. [49] noticed that microvoiding in stretched iPP tapes take place already at $\lambda = 10$. In the study of Alcock et al. [48] at $\lambda = 17$ the density reached 0.73 gcm^{-3} which means an almost 20% reduction compared to the undrawn tape. PP tapes is possessed ~15 GPa tensile modulus and ~450 MPa tensile strength by high drawn ratio (λ=17).

Hot compaction

Ward et al. [50, 51] developed a new method to produce SRPCs, which they called "hot compaction". The related research started with highly oriented PE fibers and tapes. When these preforms were put under pressure and the temperature increased their surface and core showed different melting behaviors. This finding was exploited to melt the outer layer of the fibers and tapes, which after solidification (crystallization) became the matrix. The residual part of the fibers and tapes (i.e. their core section) acted as the reinforcement in the resulting SRPC – cf. Figure 8.
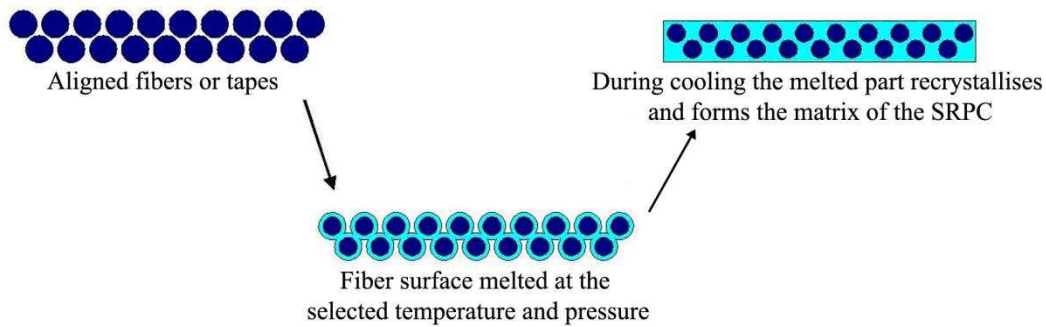
Figure 8: Principle sketch of hot compaction on the example of unidirectional (UD) arranged fibers

It was found that hot compaction works well for semicrystalline, liquid crystalline and amorphous thermoplastics, as well [52]. By hot compaction different high-strength SRPMs were produced from of PET [53, 54], PE [55, 56], PEN [52], PA-6.6 [57], PPS [52], POM [58], PP [59], PMMA [60] and PEEK [52]. It is intuitive that the processing window during hot compaction of single-component polymeric systems is very narrow. When the compaction temperature approaches the melting temperature of the fiber, the transverse strength of composites with UD-aligned (i.e. 1D) reinforcement increases, however at cost of stiffness and strength measurable in longitudinal direction [61] (cf. Figure 9). Figure 9 also displays how narrow the temperature range for the productions of SRPMs is.
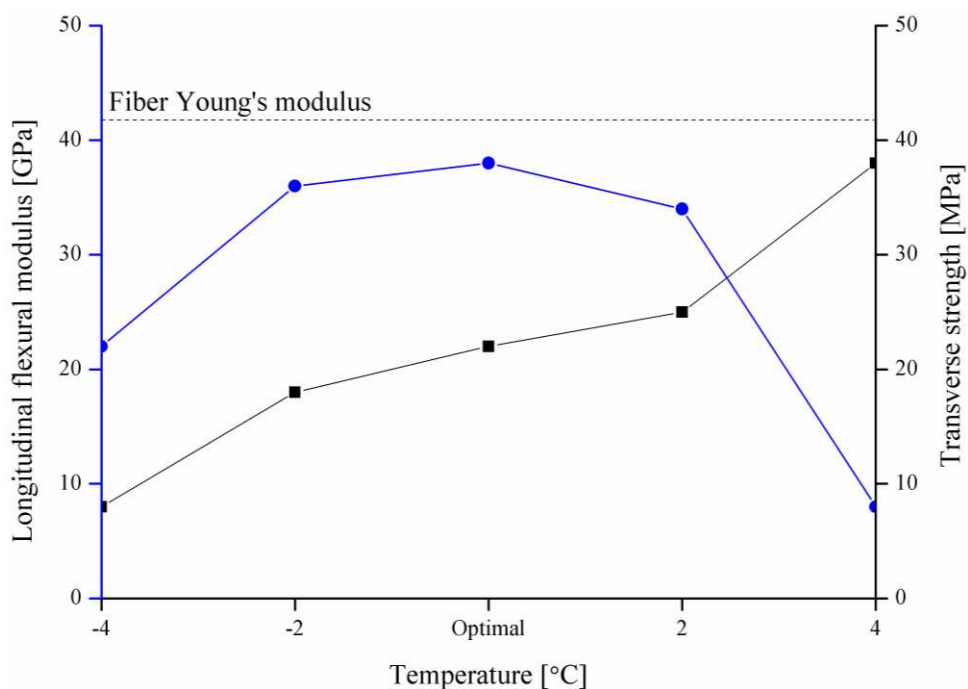
Figure 9: Longitudinal flexural modulus (●) and transverse strength (■) vs. compaction temperature of melt spun polyethylene fibers (based on [61])

19

It was also reported that in order to set optimum mechanical properties a given amount of the fiber should melt and work later as matrix. This was given by ca. 10% of the cross section (i.e. outer shell) of the fiber. This value is very closely matched with that amount which is required to fill the spatial voids between those fibers which adapt a hexagonal-like cross-section owing to the acting pressure. The hexagonal shaping of the initially spherical fibers along with the formation of a transcrystalline layer between the residual fiber (core) and matrix formed, have been proved [61]. Ratner et al. [62] experienced with an additional surface crosslinking during hot compaction of UHMWPE fibers. The surface of the fibers was coated by a solution containing a peroxide prior to the hot compaction (T=140-150°C, pressure: 31 MPa, time: 30 min). By this way the stress transfer between the residual fiber (reinforcement) and the newly formed matrix has been improved compared to non-treated versions. Probably this is the right place to draw the attention to the effect of the transcrystalline layer, the effect of which from the point of view of fiber/matrix adhesion is controversially discussed. Though the development of the transcrystalline layer is necessary, its internal build-up may be of great relevance as outlined by Karger-Kocsis [63]. Ratner et al. [64] found that the crosslinked interphase between fiber and matrix is more beneficial than the usual transcrystalline one, especially when long-term properties, like fatigue, are considered. Hine et al. [55] produced SRPMs using fabrics (i.e. 2D reinforcement) composed of high-modulus PE fibers (E-modulus: 42 GPa). It was established that with increasing hot compaction temperature the molten proportion of the fibers increased, and the crystallinity of the matrix formed became markedly less than that of the initial fibers. A further important finding was that the processing temperature for 2D fabrics is higher than for UD (1D) aligned fibers. This is due to the fact that in an assembly of woven fabrics more interstitial space has to be filled with the matrix than in a parallelized 1D fiber one. The quality of the related SRPM was measured by interlayer T-peel tests. The T-peel strength increased steeply with the matrix fraction (up to 30%) and reached a constant value afterwards. Based on tensile tests and detailed morphological studies, the authors quoted that the final matrix content should be between 20 and 30% in order to set optimum properties for SRPMs from woven fabric layers. It was also emphasized that the processing window for 2D fabrics is even smaller than for 1D fibers or tapes. However, UHMWPE is losing its stiffness and strength, and becomes prone for creep with increasing temperature. To overcome this problem the UHMWPE fibers were exposed to γ-irradiation to trigger their crosslinking [52]. Orench et al. [65] performed a comparative study on SRPMs produced from commercially available high-strength fibers and tapes (Spectra®, Dyneema®).

Due to the low temperature resistance of PE, the hot compaction research shifted to PP [59]. This direction yielded new insights, such as the PP should be kept under high pressure already during

heating to the compaction temperature to avoid its thermal shrinkage. Hine et al. [66] compacted PP tapes from fibrillated woven PP in both open and closed molds. Based on flexural tests and morphological inspection the optimum processing conditions were defined. Teckoe et al. [67] manufactured 2 mm thick sheets from woven fabrics consisting of high-strength PP fibers. The fabric layers were subjected to 2.8 MPa pressure until the compaction temperature (varied between 166 and 190°C) was reached. This temperature was kept for 10 min before rising the pressure suddenly to 7 MPa and keeping it during cooling to 100°C where demolding took place. At low compaction temperatures the voids within the woven structure were not completely filled, at high temperatures too much matrix was produced and thus the reinforcement content diminished. It was claimed that final matrix content should be between 20 and 30% for good quality products. It is worth of noting that heating of the related preform to the compaction temperature is accompanied with the release of its internal stress state. Due to the high pressure applied the material melts under constraint conditions – so its melting occurs at higher temperature than under normal conditions. This is the reason why the optimum hot compaction temperature is close, and even above, the usual melting under unconstraint conditions. Jordan and coworkers [68-70] studied the effects of hot compaction on the performance of PE, PP tapes and fabrics. The latter differed in their mean molecular weight, which influenced the consolidation quality, assessed by tear tests. Bozec and coworkers [71] investigated the thermal expansion of self-reinforced PE and PP containing 2D (i.e. woven fabric) reinforcements. Good quality products were received at the following conditions – PE: p=0.75 MPa, T=139°C; PP: p=3 MPa and T=183°C. The shrinkage, E-modulus and linear thermal expansion coefficient of the corresponding SRPMs were determined. It was reported that especially the PP systems were sensitive to changes in the compaction conditions. Hine and coworkers [72] devoted a study to check whether the insertion of film layers between the fabrics to be compacted results in improved consolidation quality, and whether this "interleaving concept" can widen the temperature window of the processing. Note that this method is basically a combination of hot compaction and film stacking (to be disclosed later). This strategy yielded the expected results: the consolidation quality was improved (well reflected in the mechanical property profile), the interlayer tear strength enhanced, and the processing temperature interval enlarged. This approach was also followed for PP fibers. In a further study Hine et al. [73] incorporated carbon nanofiber (CNF up to 20 wt%) to improve the reinforcing activity of the PP preform after hot compacted. The small amounts of CNF significantly improved the properties of isotropic PP. For example, adding CNF in 5 vol% increased the Young's modulus at the room temperature by 60% and reduced the thermal expansion coefficient by 35%. Attempts were also made to improve the bonding between CNF and PP via oxygen plasma

treatment of the CNF (less successful) and using a maleic anhydride grafted compatibilizer for PP (more successful).

McKown and Cantwell [74] studied the strain-rate sensitivity of a hot-compacted self-reinforced PP composite. The SRPP specimens were subjected to strain-rates ranging from 10^{-4} s^{-1} to 10 s^{-1}. The SRPP composite showed similar characteristics to the neat PP material in respect to the stress–strain behavior with increasing strain-rate. Stiffening of the material in the elastic region was followed by enhanced yield stress and maximum stress with increasing strain rate. Parallel to that the strain-to-failure was reduced. The failure mode of the SRPP composite was characterized by longitudinal fiber fracture with varying degree of inter-ply delamination over the dynamic tensile loading range studied.

Prosser et al. [75] investigated the termoformability of hot compacted PP sheets with 2D reinforcement (woven fabric). It was reported that the self-reinforced PP sheets experienced considerable work hardening according to in-plane tensile tests performed at high temperatures- cf. Figure 10.
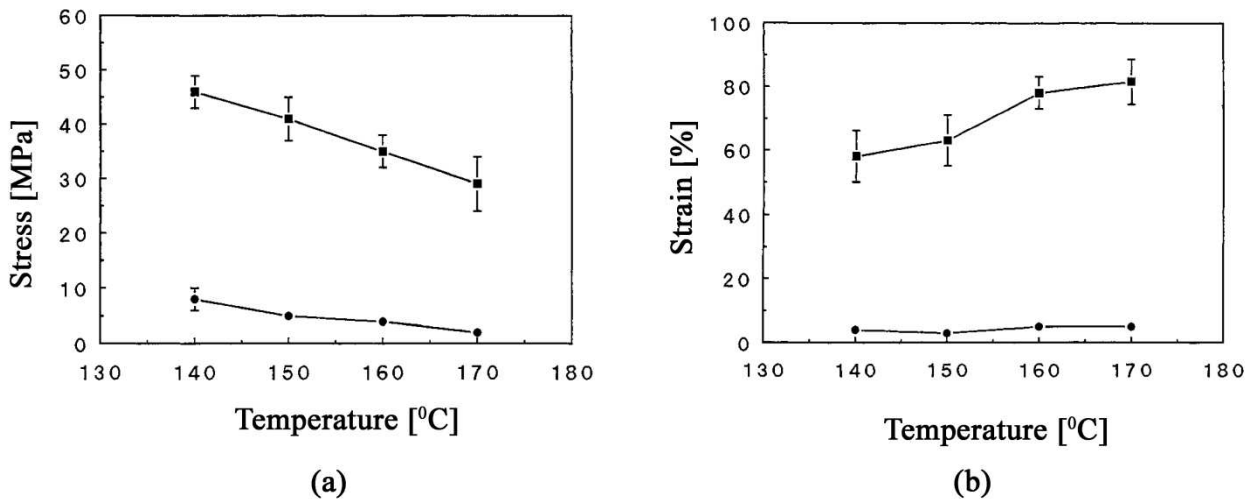

Figure 10: Effects of testing temperature on the stress-strain behavior of self-reinforced PP with 2D reinforcement, schematically. (a) Dependence of yield strain (●) and failure strain (■) as a function of temperature; (b) dependence of yield stress (●) and failure stress (■) as a function of temperature [75]

The authors observed that the optimum thermoforming temperature is very close to that of the melting of the matrix that was formed by recrystallization of the molten part of the parent fiber/tape. Romhány et al. [76] studied the fracture and failure behavior of woven fabric reinforced self-

reinforced PP (Curv®) making use fracture mechanical concepts and recording the acoustic emission during loading of the specimens. The latter technique proved to be well suited to characterize the consolidation quality. Jenkins et al. [77] prepared a range of flat hot-compacted single-polymer composite panels from oriented PP and PE. The panels differed in their dynamic modulus and damping capacity values. SRPMs were subjected to mechanical excitation, allowing their acoustic frequency response over the audio bandwidth to be measured. The results showed that the correlation of mechanical and acoustic frequency response functions with the dynamic modulus, damping, and specific modulus of the panel materials. The ideal combination of material properties to maximize the acoustic output of the panels was given by: high stiffness and low density to reduce the impedance of the panel and low damping to enhance the efficiency.

Major goal of the hot compaction technology was to offer lightweight and easy recyclable thermoplastic composites to the transportation sector. As further application fields sporting goods, safety helmets, covers and shells (also for luggage) were identified. Hot compacted PP sheets from woven PP fabrics are marketed under the trade name of Curv® (www.curvonline.com).

As mentioned before, the hot compaction method was successfully transferred to many other polymers, like multifilament assemblies of PET and PEN [53, 78], PA-6.6 [57], POM and PPS [52], PEEK [52], and even for PMMA [60]. Needless to say that the optimum compaction conditions are strongly material-dependent.

Production by film stacking

During film stacking the reinforcing layers are sandwiched in between the matrix-giving film layers before the whole "package" is subjected to hot pressing. Under heat and pressure the matrix-giving material, having lower melting temperature than the reinforcement, melts and infiltrates the reinforcing structure accordingly. Recall that both matrix and reinforcement are given by the same polymer or polymer family. The film stacking procedure is highlighted in Figure 11.
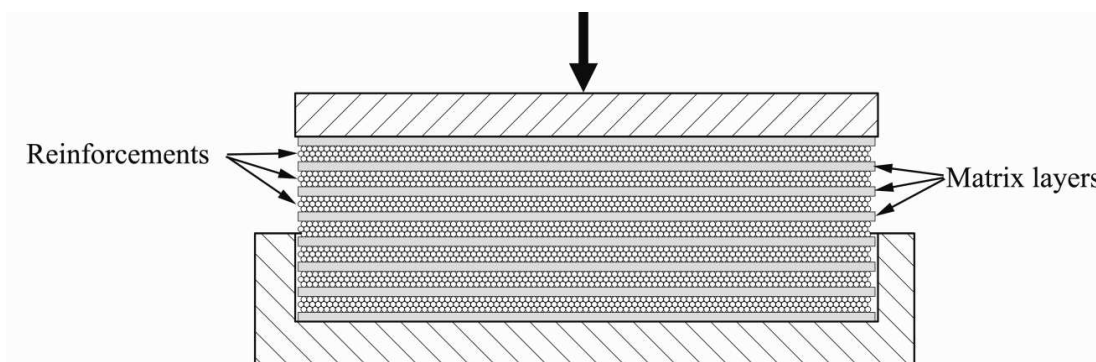

Figure 11: Scheme of the composite processing via film stacking

The necessary difference in the melting temperatures between matrix and reinforcement can be set by using different polymer grades (e.g. copolymer for the matrix and homopolymer for the

reinforcement – which per definition belongs to the multi-component SRPMs) or polymorphs (e.g. lower melting modification for the matrix and higher melting one for the reinforcement – this concept yields a single-component SRPM). It is of great importance to have a large enough temperature range between the melting temperature of the composite constituents. Accordingly, the matrix-forming grade melts and wets out of the reinforcing structure without causing a temperature-induced degradation in the stiffness and strength of the reinforcement, or at least keeping it in an acceptable level. Those thermoplastic systems, which can be used to produce single- and multi-component SRPMs via film stacking, are summarized in Table 2.

Composite	Matrix	Reinforcement	Processing temperature range (ΔT)
■ PE	LDPE	UHMWPE fiber	20-40°C
	HDPE	UHMWPE fiber	20-40°C
■ PP	β-PP*	highly oriented iPP fiber	20°C
	random PP copolymer	highly oriented iPP fiber	25°C
	iPP*	highly oriented iPP fiber	8-10°C
■ Polyester	PETG	PET fiber	40-60°C
	PETG	PEN fiber	15-20°C
	CBT^x	PBT	60-80°C
■ LCP	LCP	LCP (Vectran® M)	25°C

Table 2 Possible polymer pairs to produce SRPMs; * single component SRPM; × production occurs via liquid composite molding.

In the follow-up section we shall treat only the single-component SRPM versions. Bárány et al. [79-82] produced different PP-based SRPMs. For reinforcement highly oriented fibers in different textile architectures (carded mat, carded and needle-punched mat, in-laid fibers in knitted fabrics), whereas for matrices either PP fiber of lower orientation (the same textile assemblies as indicated above) or beta-nucleated PP films were selected. Note that some of the above preforms do not even contain interleaving films and thus do not fall strictly under the heading of film stacking. The matrix-giving phase in them is either discontinues fiber or a knitted fabric. Nevertheless, their consolidation occurred by hot pressing as in case of film stacking. It should be born in mind that the melting temperature of the beta-modification of isotactic PP is >20^{0}C lower than the usual alpha-form [83]. The beta-modification can be achieved by incorporating selective beta nucleating agent in the PP through melt compounding [84]. The concept of this alpha(reinforcement)/beta(matrix) combination should be credited to Karger-Kocsis [85].

The consolidation quality of the all-PP composites produced by Bárány et al. [86] was mostly studied as a function of processing conditions, viz. temperature. With increasing temperature the stiffness

and strength increased and the resistance to out-of-plane type perforation impact reduced. The consolidation quality of the layered composite laminates could be well qualified by the interlaminar tear strength. Bárány et al. [80, 81] used later PP fabric (woven type from split yarns) as reinforcement and beta-nucleated PP film as matrix giving material. As mentioned above, the benefit of the beta-modification is the widening of the melting temperature range between reinforcement and matrix [87]. With increasing processing (pressing) temperature the consolidation quality was improved. Parallel to that, the density, tensile and flexural stiffness and strength increased, whereas the penetration impact resistance diminished. The authors proved by polarized light microscopy the presence of transcrystalline layer between the PP reinforcement and PP matrix – cf. Figure 12.
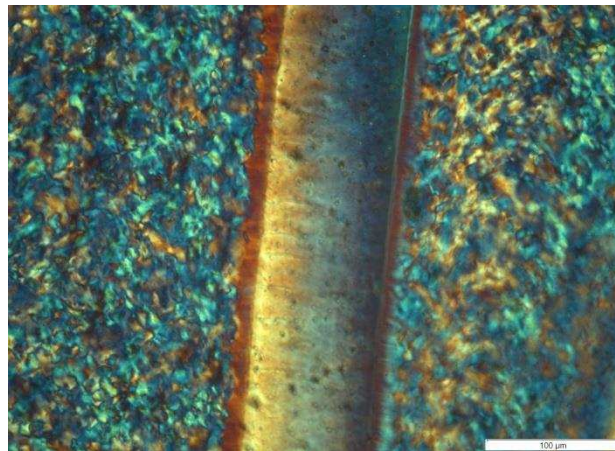

Figure 12: Transcrystalline layer between PP fiber and β-rPP matrix

Izer and Bárány [82] manufactured all-PP composites by direct hot pressing of suitable textile assemblies. As indicated above, these assemblies contained both the reinforcement and matrix giving phases in form of fibers with different orientation (draw ratio). Recall that the latter is the guarantee for a small difference in their melting temperatures that was used in this case. Abraham et al. [88] produced all-PP composites with tape reinforcement by exploiting the difference in the melting behavior of the alpha- and beta-polymorphs. The alpha-PP tapes were arranged in UD and cross-ply (CP) manner by winding whereby putting beta-nucleated PP films in between the related reinforcing tape layers. The stiffness as a function of temperature of the corresponding composites was determined by dynamic mechanical thermal analysis (DMTA).

Bhattacharyya et al. [89] prepared SRPM by combining hot compaction and film stacking. High tenacity PA6 yarn as a reinforcement and PA6 film from pellet as matrix were used. The yarn was subjected to annealing in vacuum (3 h at 150°C) in order to get higher melting point. Two yarn layers was sandwiched between two matrix films and subjected to compression molding at 200°C for 5 min under a pressure of 15 MPa. With combining of these two techniques good wetting properties were achieved and materials with excellent mechanical properties produced. The tensile modulus and

strength of the composites were improved by 200% and 300-400%, respectively, compared to the initial isotropic matrix film.

Num.	Process	Materials	Processing conditions	Results	Comment	Ref.
1	Ram extrusion	HDPE	Entrance semi-angel of 30°, p=40…110 MPa, T= 90…120°C	E_t=0.2…0.9 GPa	high friction, low extrusion rates	[24]
		HDPE	p=0…100 MPa, λ=3.75…6, T=105°C	E_t=1.1 GPa, k=0.4…0.5 W/mK	thermal relaxation after leaving the die	[26]
		PP	p=0…100 MPa, λ=3,75…6 , T=130°C	E_t=1.7 GPa, k=0.1 W/mK	lubrication applied	[26]
2	Hydrostatic extrusion	UHMPE	v=1…50 cm/min, p=0…250 MPa	E_t=10…60 GPa	batch process	[24]
3	Die-drawing	HMWPE	λ=1…13, T=115°C	λ=1…7 elongated spherulites λ=7…12 lamella structure	decreased creep	[27]
		PP	λ=6…11, T=200°C	E_t=1…12 GPa	increased tenacity	[28, 29]
		POM	Entrance semi-angel of 5…20°, λ=1…16	E_B=3…26 GPa	increased crystallinity	[30]
4	Super drawing	PTFE	λ=6…160	E_t=38…102 GPa, $σ_B$=0.7…1.4 GPa	increased crystallinity	[31]
5	Rolling	HDPE	λ=2…9	E_t=3…15 GPa, $σ_B$=30…290 MPa	increased crystallinity	[24, 34-36]
		PP	λ=2…9	E_t=4…10 GPa, $σ_B$=30…350 MPa	increased crystallinity	[24, 37]
6	Gel drawing	UHMWPE	λ=3…22	E_t=10…90 GPa, $σ_B$=0.3…3.5 GPa	increased crystallinity	[40-42]
7	Orientation drawing	HDPE	T_D=110…120°C, λ=5.8…30	E_t=6…35 GPa, $σ_B$=250…1200 MPa	micro-cracking	[43, 44]
		iPP	T_D=163…164°C, λ=21.5…35.5	E_t=18.5…24.7 GPa, $σ_B$=0,6…1.1 GPa	physical aging	[45]
8	Hot compaction	UHMPE*	T_{proc}=134…154°C, p=0.7-21 MPa	E_t=9.9…85 GPa, $σ_B$=200 MPa	unidirectional, woven structure	[52, 55, 56, 61, 65, 68]
		UHMWPE	T_{proc}=145°C, p=31-49 MPa	E_t=0.4 GPa, $σ_B$=3.7 MPa	crosslinked	[62, 64]
		PP*	T_{proc}=164…195°C, p=1.1-14 MPa	E_t=1.6…3.9 GPa, $σ_B$=25…168 MPa	high acoustic output	[59, 66, 69-72, 74-77]
		PET	T_{proc}=249…256°C, p=1.9-32.4 MPa	E_t=11.5 …13 GPa, $σ_{B,T}$=15…35 MPa	good adhesion	[53]
		PEN	T_{proc}=268…276°C,	E_t=2…. 9.6 GPa, $σ_B$=22…207 MPa	0/90 multifilament	[52, 78]
		PA-6.6	p=2.8 MPa	E_t=4.1 GPa, $σ_B$=50 MPa	woven structure	[57]
		PPS	$T_{proc,opt}$=288°C,	E_t=5.2 GPa, $σ_B$=80 MPa	chemical resistance	[52]
		PP/CNF	T_{proc}=230°C, T_{mold}=190°C	E_t=1.5…2.7 GPa	2, 4, 6, 10, 20 wt% of CNF	[73]
		POM	$T_{proc,opt}$=182°C	E_t=1.9…5.3 GPa,	POM powder	[58]
		PMMA	T_{proc}=100…125°C	$σ_B$ =65…165 MPa	unidirectional structure	[60]
		PEEK	$T_{proc,opt}$=347°C	E_t=3.65 GPa ,$σ_B$=100 MPa	woven structure	[52]
9	Film-stacking	β-PP/α-iPP	T_{proc}=150…170°C, p=7 MPa	$E_{t,L}$=2.4…2.7 GPa, $σ_{B,L}$=20…100 MPa $E_{t,T}$=1.6…2.4 GPa, $σ_{B,T}$=20…43 MPa	carded needle-punched mat	[79]
		β-PP/PP	T_{proc}= 156…186°C, p=7 MPa	E_t=2.5…3 GPa, $σ_Y$=90…100 MPa	PP woven textile	[80, 81]
		iPP/iPP	T_{proc}=160…170°C, p=6 MPa	E_t=2.1…2.5 GPa, $σ_B$=29…140MPa	knitted, carded and needle punched mats	[82]
		β-PP/α-PP	T_{proc}=160°C, p=7 MPa	E_t=2.3 GPa, $σ_B$=60 MPa	winding	[88]

Table 3: Production methods, conditions and product characteristics of single-component SRPMs produced in multi-step (ex situ) (*summarized results)

2.2 Multi-component SRPMs

SRPMs can also be produced by the combination of such polymers which belong to the same family of polymeric materials. The major goal during their preparation is to achieve a good adhesion (bonding) between the reinforcing and matrix-giving polymer phases. Like to the single-component SRPMs, the reinforcing structure may be generated in single- (in situ) or multi-step (ex situ) operations. Accordingly, a similar grouping as before can also be followed here. Next the different variants will be introduced briefly.

2.2.1 Single-step production

Multi-component extrusion yielding self-reinforced structure

The extrusion die with convergent section allow us to set a unidirectional (1D) molecular alignment in situ which will work as reinforcement owing to the supermolecular structure formed by crystallization. Chen et al. [90] solved, however, the problem of biaxial orientation (2D) by using a specially designed fish-tail shaped (bi-cuneal shape) extrusion die as depicted in Figure 13.
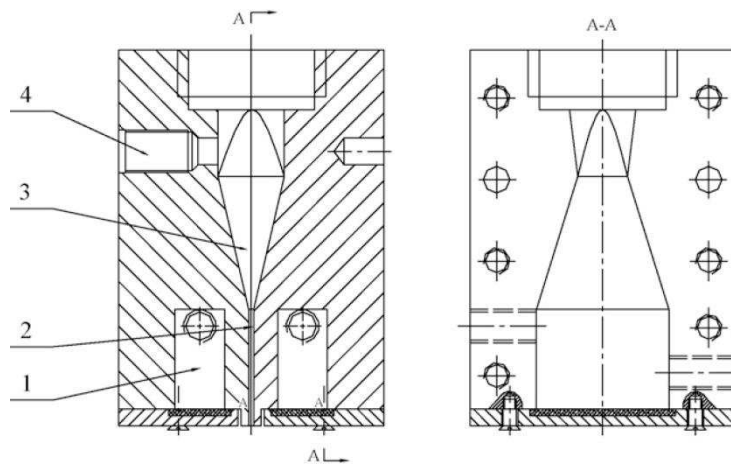

Figure 13: Schematic representation of the self-reinforcing sheet extrusion die: (1) temperature controlling oil bath, (2) the straight section, (3), the convergent section, and (4) double functional temperature–pressure sensor [90]. "Reprinted from Journal of Materials Processing Technology, 202, Chen J., Yang W., Yu G. P., Wang M., Ni H. Y., Shen K. Z.: Continuous extrusion and tensile strength of self-reinforced HDPE/UHMWPE sheet., 165-169., Copyright (2010), with permission from Elsevier"

Composites with planar reinforcement were produced via this die from HDPE and HDPE/UHMWPE blends using a single-screw extruder. The mold was oil tempered (T=126-137℃) and the optimum processing pressure was between 15 and 30 MPa. Under conventional extrusion conditions the tensile

strength of extruded sheet was comparable to conventional molded HDPE samples. The tensile strength was almost the same in both machine (MD) and transverse directions (TD). The tensile strength of the HDPE/UHMWPE in extrusion and transverse directions, respectively, were 6 and 3 times higher than those of the related sheet produced traditionally (HDPE).

Multi-component SCORIM/OPIM

Zhang et al. [91, 92] processed LDPE/HDPE and HDPE/PP blends by the earlier introduced OPIM technique (oscillation frequency: 0.3 Hz). It was established that with increasing LDPE content the tensile strength diminishes, whereas the toughness increases for the LDPE/HDPE blends. Morphological studies confirmed the onset of a shish-kebab type supermolecular structure. The tensile strength of the HDPE/PP blends could also be markedly increased (fivefold) when the PP content remained below 10 wt%. Zhang et al. [93] investigated the performance of HDPE/UHMWPE when processed by the SCORIM technique. Tribological tests showed that the wear resistance of the related system was ca. 50% better than that of traditionally molded specimen.

Num.	Processing	Materials	Processing conditions	Results	Comment	Ref.
1	**Self-reinforced extrusion**	HDPE/UHMWPE	T_{proc}=125-180°C, p=2…30 MPa	σ_B=20…170 MPa	specially designed fish-tail shaped extrusion die	[90]
2	**SCORIM/ OPIM**	HDPE/LDPE	T_{melt}=200°C p_{proc}=90 MPa T_{mold}=25°C	σ_B=21…109 MPa	shish-kebab structure (WAXD)	[91]
		HDPE/PP	T_{melt}=220°C p_{proc}=32…48 MPa T_{mold}=42°C	σ_B=25…90 MPa	(< 10 wt% PP)	[92]
		HDPE/UHMWPE	-	μ=0.3…0.5 (0.3) Load-carrying capacity= 70 N (35 N)	micro-cracks parallel to the surface (conventional packing)	[93]

Table 4: Production methods, conditions and product characteristics of multi-component SRPMs produced in single-step (in situ)

2.2.2 Multi-step production

The first publication of this processing version should be credited to Capiati and Porter [94]. They combined HDPEs with different melting characteristics. The high-modulus fibers (reinforcement) melted at 140, while the matrix-giving HDPE at 131°C. The HDPE fiber was embedded in the molten HDPE using a special rheometer. After cooling/solidification the fiber in this single fiber reinforced composite was subjected to pull-out test. It was reported that the interfacial shear strength is comparable with that of the glass fiber/epoxy system. Moreover, the presence of transcrystalline layer was detected at the fiber/matrix surface.

Consolidation of coextruded tapes

The development of SRPMs is best reflected by searching for options which amplify the difference between the melting of the reinforcement and matrix. Recall that this range was highly limited for hot compaction. Peijs et al. [95] developed a coextrusion technique via which the melting temperature difference between the composite constituents reached 20-30°C. The invention was to "coat" a PP homopolymer tape from both sides by a copolymer through a continuous coextrusion process. Note that a copolymer melts always at lower temperature than the corresponding homopolymer owing to its less regular molecular structure. The coextruded tape was stretched additionally in two-steps – cf. Figure 14. This resulted in high-modulus, high-strength tapes.
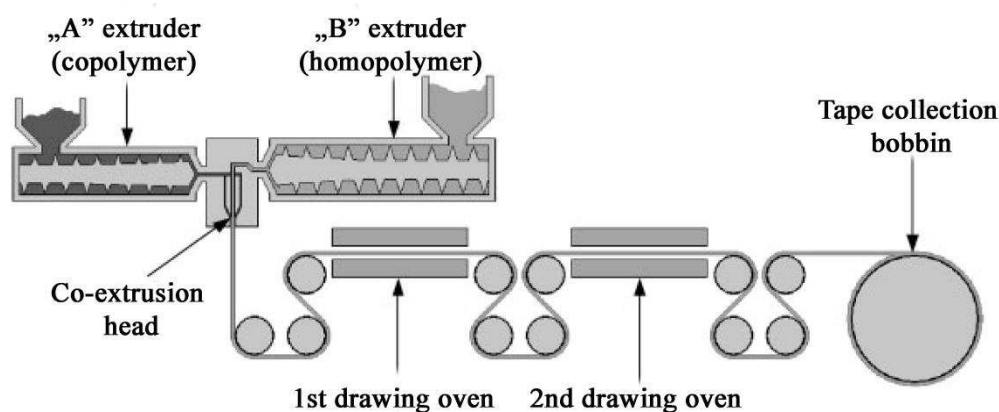

Figure 14: Coextrusion technology with additional stretching to produce high-strength tapes [96] "Reprinted from Journal of Applied Polymer Science, 104, Alcock B., Cabrera N. O., Barkoula N. M., Loos J., Peijs T.: Interfacial properties of highly oriented coextruded polypropylene tapes for the creation of recyclable all-polypropylene composites., 118-129. Copyright (2010), with permission from John Wiley and Sons"

The primary tapes could be assembled in different ways: as in composite laminates (ply by ply structure with different tape orientation, such as UD /cf. Figure15/ and CP) or integrated in various

textile structures (e.g. woven fabrics). The consolidation of the related assemblies occurred by hot pressing.
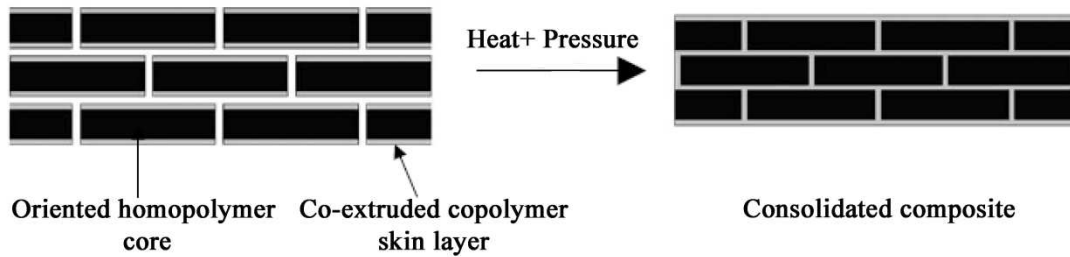

Figure 15: Production of composites with UD tape alignment from coextruded tapes [97]

Advantage of this method is that the reinforcement (core) content of the tape may be as high as ca. 80%. This, along with the high draw ratio yielded tapes of excellent mechanical properties (E-modulus >6 GPa, tensile strength >200 MPa). Cabrera et al. [97] prepared all-PP composites from UD and woven fabric assemblies of coextruded tapes. For the consolidation of the UD composites 17 MPa pressure was used and the temperature covered the range between 140 and 170°C. The time was kept constant (15 min) during hot pressing. The E-modulus of the laminates, measured both in tape direction and transverse to it, was not much affected by the processing temperature. By contrast, the interlaminar tear strength was improved by increasing temperature, well reflecting the improvement in the consolidation quality. The woven fabric-reinforced composites were subjected to falling dart (perforation impact) tests. Based on the related specific (i.e. thickness-related) perforation impact energy data the all-PP composites outperformed both the glass fiber (GF) mat (three times higher) and flax mat-reinforced counterparts (six times higher). Alcock et al. [98] manufactured UD composite sheets by winding the coextruded tapes on a metallic frame which was put later in between the plates of a press operated in the temperature interval T=140 to 160°C. The properties of the composites were determined in mechanical, whereas the reinforcement content (reaching 90 wt%) via microscopic investigations. As usual for all UD-reinforced composites, both the tensile E-modulus and strength decreased with increasing angle between the reinforcing and loading directions (off-set) during their testing. The transverse compressive strength (10 MPa) was not affected by the pressing temperature. The results received were compared with those measured on 50 wt% UD GF-reinforced PP composites. Albeit the UD-GF PP composite preformed better than the all-PP, the latter took the leading in respect to the related specific (i.e. density-related) properties. In follow-up studies Alcock et al. [96, 99-102] investigated the structure-property relationships in all-PP composites produced from woven fabrics composed of coextruded tapes. When the consolidation took place at low temperature (T=125°C) and under low pressure (p=0.1 MPa), the sheets exhibited excellent

resistance to perforation impact. This was traced to an intensive delamination between the fabric layers that was triggered during this high-speed perforation process. Up to 2 mm sheet thickness, the perforation energy increased linearly with the sheet thickness. Ballistic test results confirmed that the performance of composites sheets from Pure® tapes is comparable with that of the state-of-art ballistic materials. The authors draw the attention to the fact, that the mechanical performance of the all-PP composites, containing fabrics of coextruded tapes, can be optimized upon request by selecting suitable textile architectures and hot pressing/consolidation parameters (pressure, temperature). Barkoula et al. [103] investigated the fatigue performance of PP tapes and woven tape fabric reinforced all-PP composites. It was found the endurance limit (or fatigue threshold, below which no fatigue-induced property reduction occurs), controlled by the onset of delimitation, is strongly affected by the processing temperature. The fatigue threshold of the optimum processed composite was at 65% of the static tensile strength. This is markedly higher than of GF mat-reinforced PP-composites showing a range of 30-40% [104].

Banik et al. [105, 106] studied the short-term creep performance of coextruded tape-reinforced PP composites with both UD- and CP-type tape lay-ups. The related sheets were produced by vacuum bagging in an autoclave (which is almost exclusively used for thermoset composite production) under 2.4 MPa pressure and at T=138°C. The flexural creep tests were performed in a DMTA device in the temperature range of 20 to 80°C. It was reported that the creep depends on the composite lay-up. By adopting the temperature-time superposition principle to the short-term creep results a master curve was constructed that predicted the long-term creep at a given temperature. Kim et al. [107] studied also the creep response of all-PP composites and emphasized that small changes in the processing conditions have a pronounced effect on the creep behavior. It is noteworthy that composites from coextruded PP tapes in different assemblies were produced by various techniques, such as hot pressing, tape-winding [108], stamp forming, vacuum bag/autoclave [109, 110]. Moreover, the related sheets were used for face covering of different sandwich structures with cores including honeycomb structures and foams. The face sheeting occurred with or without additional primer [111]. Recall that the coextruded PP tapes are known under the trade name of Pure® and Armordon® (www.pure-composites.com; www.armordon.com).

Film stacking

This technique is usually used for such SRPMs the constituents of which are from the same polymer family. Shalom et al. [112] produced high-strength PE fiber (Spectra®) reinforced HDPE composites by winding the fiber unidirectional and sandwiching HDPE films in between the wound fiber layers. The reinforcing fiber content in the UD assembly was 80 wt%. Its consolidation occurred by hot

pressing (T=137⁰C, p=16.5 MPa). Coupon samples were subjected to tensile tests whereby varying the loading direction in respect to the UD fiber alignment (off-axis tests). As expected, the E-modulus, yield strength and resistance to fracture were the higher the smaller the off-axis angle was. Houshyar et al. [113] used a mat from PP homopolymer fibers as reinforcement (fixed at 50 wt%), and PP copolymer film as matrix-giving material. The difference in their melting temperature was ca. 16⁰C according to DSC results. The fiber diameter in the mat was varied. The hot consolidation occurred between 155 and 160⁰C. It was found that with increasing diameter of the mat fibers increased both stiffness and strength of the composites. The surface of the homopolymer PP fiber acted as heterogeneous nucleator and initiated transcrystalline growth. In follow-up studies [114, 115] it was demonstrated that with increasing diameter of the reinforcing PP fiber the void content in the composite can be reduced. Maximum strength was reached when the diameter of the fiber was ca. 50 micrometer. The creep results of the related composites, which were also modeled by the Burgers model, demonstrated that increasing reinforcing fiber content was accompanied with increasing resistance to creep. Object of further studies of the group of Shanks [116, 117] was to deduce possible effects of different textile architectures (covering both non-woven and woven ones) on the mechanical properties of the related all-PP composites. During the consolidation they were subjected to a low pressure (ca. 0.01 MPa) at T=158⁰C for 15 min. The mechanical results showed that the properties of the woven composites strongly depend on the woven geometry. The composite with satin cloth delivered the best properties. This was due to the advantages of the satin parameters, such as long float length, high fiber count, few interlace points and loose pattern.

It is noteworthy that the authors used the term "compaction" though this is reserved for those techniques in which a part of the reinforcing phase becomes molten and thus overtaking the role of the matrix after cooling. This is not the case in film stacking where the melting temperature of the reinforcing fiber or tape is usually not surpassed. In order to improve the energy absorption capability of the resulting composites, Houshyar et al. [118] modified the matrix. This was done by extrusion melt compounding of the matrix-giving PP copolymer with ethylene-propylene rubber (EPR; up to 30 wt%) with follow-up sheeting.

Houshyar et al. [119] modeled the PP fiber-matrix composites with finite element analysis. The model demonstrated that the stress concentration at the fiber-matrix interface increased with decreasing fiber content. The ratio between matrix and fiber stiffness was significant and the interfacial stress carried by both constituents acted to reduce the risk of premature interfacial failure and increased the mechanical properties of the composite. The finite element model showed that at low fiber content, the fiber was not able to share a larger portion of applied stress. The matrix carried

the main portion of stress and yielded in a large scale when the applied stress reached the matrix strength.

Bárány et al. [120] prepared composites using random PP copolymer films and carded and needled punched mats as matrix and reinforcing phases, respectively. The nominal reinforcement content was 50 wt%. The consolidation was performed at different temperatures in the range of T=150-165°C. Consolidation at 150°C resulted in poor performance, whereas above T=165°C did not yield additional property improvement. Bárány et al. [80, 81] studied also the perforation impact resistance of all-PP composites containing woven fabrics from split flat yarns as reinforcement, and films composed of both alpha and beta-phase random PP copolymers as matrix-giving materials. The beta-modification was produced by using selective beta-nucleant. The perforation impact resistance of the composite with beta-nucleated random PP copolymer was higher that the alpha-variant. Bárány and Izer [121] estimated the long-term flexural creep of self-reinforced polypropylene composites based on short-term creep tests performed at different temperatures. An Arrhenius type relationship was used for shifting the related creep data along the time axis. It was found that with improved consolidation (increasing processing temperature) the creep compliance decreased. Moreover, good correlations were found between the creep compliance and density, and between the creep compliance and interlayer peel strength.

Abraham et al. [88] produced high-strength alpha PP homopolymer tapes by a single-step hot stretching and used this as UD or CP reinforcement in alpha- and beta-phase random PP copolymer matrices. The interphase between the reinforcement and matrix was composed of a transcrystalline layer, which was larger in the beta- than in the alpha-phase random PP copolymer matrix. This finding was traced to the fact that the composite with beta-nucleated matrix performed better than the alpha version.

Kitayama et al. [122] produced SRPMs from PP homopolymer fiber (reinforcement) and random PP copolymer (matrix) by film stacking and studied the interphase formed. Here a transcrystalline layer was resolved, the structure of which changed with the consolidation temperature – cf. Figure 16.
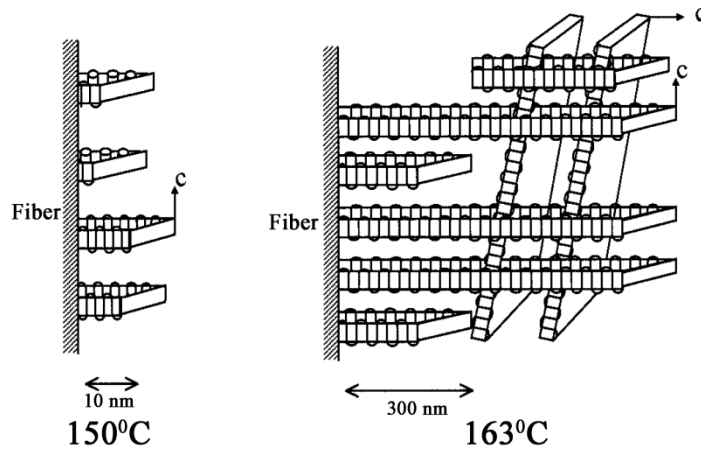
Figure 16: Lamellar structure within the transcrystalline layer as a function of the consolidation temperature [122]

The lamellar structure, depicted in Figure 16, can be stretched upon loading without its detaching from the surface of the reinforcing PP homopolymer fiber, which is very beneficial in composites. Recall that the lamellar structuring in the transcrystalline layer for optimum stress transfer from the matrix toward the fiber, proposed by Karger-Kocsis et al. [123], is very similar to that in Figure 16 (cf. Figure 17).
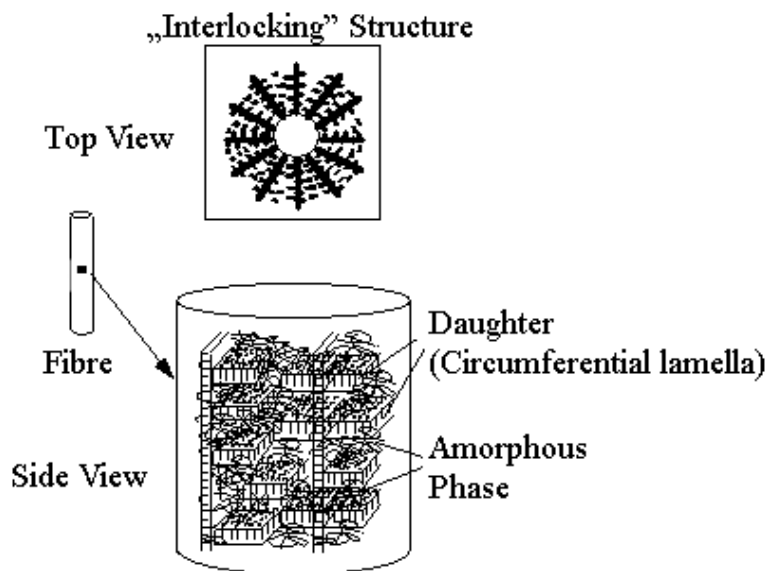

Figure 17: Hypothesized interphase with lamellar interlocking and amorphous phase as adherent for the transcrystaline layer initiated by flat-on type lamellar growth on fiber surface [123]

Ruan et al. [125] manufactured nanoparticle filled self-reinforced PP composites, where they used fumed SiO_2 as nanoparticle. The nanoparticles were preheated at 140°C under vacuum for 5 h. Then the mixture of monomer (butyl acrylate) and the nanoparticles and a certain amount of solvent was irradiated by 60Co γ-ray in air at a dose rate of 80 kGy. The resultant, poly(butyl acrylate) (PBA) grafted nano-SiO_2 (SiO_2-g-PBA) with a percent grafting of 3.35%, was used for the subsequent composites manufacturing. Untreated or treated nano-silica was melt compounded with iPP at 180°C in the mixer. The content of nano-silica in all the composites is 1.36 vol%. The sheets of SiO_2/PP was produced by hot pressing, and then the sheets were hot drawn under a temperature slight lower than the melt temperature of PP (150°C) at a constant velocity. Film with a thickness of 50 μm was blown from the random PP copolymer by film blowing. Finally, the stretched sheets were film-stacked with copolymer films by a specially designed mold and were hot pressed at different processing temperature (T=150-175°C) and under holding pressure (2.0-5.0 MPa) for constant holding time of 10 min. According to the mechanical properties reported the incorporation of nanoparticles into polymer matrix improved the mechanical properties of self-reinforced composites.

Pegoretti et al. [126-128] used thermoplastic liquid crystalline polyester fibers for both reinforcement (Vectran® HS, T_{melt}=330°C) and matrix (Vectran®M, T_{melt}=276°C). Unidirectional composites were prepared in a two stages process. At first, both Vectran®M and HS as received fibers tows were wound on an open metal frame and after the wounded LCP consolidated in hot press. As optimum processing temperature T=275°C was deduced which was associated with the lowest void content and highest mechanical strength.

Microfibrillar reinforced composites (MFC)

MFCs is a polymer-polymer composites the constituents of which are incompatible with each other, and they possess different melting temperatures. In MFCs the reinforcing microfibrils are given by "flexible" macromolecules which have been aligned during the production. Essential stages of MFC preparation are as follows: blending, extrusion, drawing and annealing. The latter occurs at a constant strain above the T_m of the component that melts at lower temperature. MFCs are usually made of condensation (PET, PA66) polymers, working as reinforcements, and polyolefins (PP, PE) acting as matrices. MFCs from PP/PE, PET/PE, PET/PP, PA-66/PP, and PA-66/PE blends (note that in the above list some reinforcement/matrix combinations are highlighted) exhibited a pronounced improvement in the mechanical properties compared to those of the respective isotropic matrix. The

mechanical properties of MFC are similar to those of short glass fiber reinforced composites containing the same matrix [129].

Num.	Processing	Materials	Processing conditions	Results	Comment	Ref.
2	**Coextrusion**	rPP/PP	T_{proc}=140, 160°C, p=2.4 MPa, λ=17	$\sigma_{B,L}$=385 MPa, $E_{t,L}$=13 GPa $\sigma_{B,T}$=5 MPa, $E_{t,T}$=1.5GPa	unidirectional structure	[98]
		rPP/PP	T_{proc}=140…170°C, p=17 MPa, λ=16	σ_F=205 MPa, E_B= 6 GPa	woven structure	[97]
		rPP/PP	T_{proc}=140°C, p=1-15 MPa, λ= 17	σ_B=20…230 MPa, E_t=2…7 GPa	woven structure, increasing impact-energy absorption	[99-102]
		rPP/PP	T_{proc}=145°C, p=2.4 MPa	σ_F=90…160 MPa, E_B=3…12 GPa	consolidation in vacuum bag (UD, 0/90 structure)	[105, 106]
3	**Film-stacking**	HDPE/PE	T_{proc}=137°C, p=16.5 MPa	σ_Y=34…190 MPa, E_t=2…7 GPa	winding angels (30…45°)	[112]
		rPP copolymer/PP	T_{proc}=155-160°C, p=16.5 MPa	σ_Y=15…30 MPa, E_t=1.6…1.8 GPa	transcrystalline structure (light microscopy)	[113]
		rPP copolymer/PP	T_{proc}=158°C, p=11…14 kPa,	σ_B=17…26 MPa, E_t=2…3 GPa	different woven structure	[116]
		rPP copolymer-EP/PP	T_{proc}=152°C	σ_B=17…26 MPa, E_t=0.3…0.7 GPa	0…30 wt% EP	[118]
		rPP/PP	T_{proc}=147…177°C, p=7 MPa	σ_Y=110…120 MPa, E_t=2…2.5 GPa	highly stretched split PP tapes	[80, 81]
		β-rPP/ PP	T_{proc}=136…166°C, p=7 MPa	σ_Y=100…110 MPa, E_t=1.5…2 GPa	highly stretched split PP tapes	[80, 81]
		rPP/hPP	T_{proc}=150…163°C, p=1.9 MPa	σ_B=14…42 MPa, E_t=0.4…0.5 GPa	transcrystalline structure (TEM)	[122]
		LCP/LCP	T_{proc}=260…285°C, p=4.4 MPa	σ_F=24…36 MPa, E_B=36…42 GPa	unidirectional structure	[126, 127]

Table 5: Production methods, conditions and product characteristics of multi-component SRPMs produced in multi-step (ex situ)

3. OUTLOOK AND FUTURE WORK

Self-reinforced polymeric materials (SRPMs) remain under spot of interest further on. This prediction is based on the fact that SRPMs are lightweight (their density is lower than most of the traditional composites) and environmental benign (especially die to their easy recycling via reprocessing in the melt).

The R&D works with single-component SRPMs will probably focus on multi-step production methods which allow a greater freedom in shaping and design. For that purpose angular pressing, well established for metals, will be explored next [130]. However, the dream of researchers is still the single-step productions of single-component SRPMs via injection molding.

For multi-component SRPMs one can expect a fast development with one-step extrusion blow molding operations. This will be fuelled by needs for hollow containers with improved barrier properties. Among the multi-step production methods of multi-component SRPMs with loose textile assemblies, which can be consolidated and shaped simultaneously, are in favored position. There is ongoing research to develop injection-moldable multi-component SRPMs.

In respect to the matrix/reinforcement combinations amorphous/semicrystalline and semicrystalline/semicrystalline (by exploiting the melting temperature difference between polymorphs) combinations will be further investigated. The reinforcing phase will be often modified by nanofillers, especially by those which have a high aspect ratio (carbon nanotube, carbon nanofiber, graphene layers, layered silicates) to increase its stiffness, strength and thermal stability.

The feasibility of some combinations, listed in Figure 1, have yet to be checked. For example, it is of high importance whether such a polymer part can be produced in which a 3D self-reinforcing structure (for example by oriented crystallization) is generated simultaneously. In this respect novel processing techniques, allowing us very high heating and cooling rates (in hundreds of °C/min range), may be of great help. It can be prophesized that in the near future SRPMs with amorphous polymer matrix and semicrystalline reinforcing phase (using polymers that belong to the same polymer family) will be pushed forward. Differences in the tacticity resulting in semicrystalline and amorphous versions (e.g. isotactic or syndiotactic PMMA reinforcements in amorphous PMMA matrices), as well as the phenomenon of polymorphism in semi-crystalline polymers will be favored topics of related research and development activities. New SRPMs and SRPCs will be produced by combining new methods (e.g. electrospinning of fibers) with well established ones (e.g. film stacking).

4. ACKNOWLEDGEMENT

5. REFERENCES

1.   Pornnimit B., Ehrenstein G. W. Extrusion of self-reinforced polyethylene. Adv Polym Tech 1991;11:91-98

2.   Kornfield J., Kimata S., Sakurai T., Nozue Y., Kasahara T., Yamaguchi N., Karino T., Shibayama M. Molecular Aspects of Flow-Induced Crystallization of Polymers. Prog. Theor. Phys. Suppl. 2008;10-16

3.   Prox M., Pornnimit B., Varga J., Ehrenstein G. W. Thermoanalytical investigations of self-reinforced polyethylene. J Therm Anal 1990;36:1675-1684

4.   Farah M., Bretas R. E. S. Characterization of i-PP shear-induced crystallization layers developed in a slit die. J. Appl. Polym. Sci. 2004;91:3528-3541

5.   Huang H. X. Continuous extrusion of self-reinforced high density polyethylene. Polym Eng Sci 1998;38:1805-1811

6.   Huang H. X. High property high density polyethylene extrudates prepared by self-reinforcement. J Mater Sci Lett 1998;17:591-593

7.   McHugh A. J., Tree D. A., Pornnimit B., Ehrenstein G. W. Flow-induced crystallization and self-reinforcement during extrusion. Int Polym Proc 1991;6:208-211

8.   Huang H. X. Self-reinforcement of polypropylene by flow-induced crystallization during continuous extrusion. J Appl Polym Sci 1998;67:2111-2118

9.   Čermák R., Obadal M., Habrová V., Stoklasa K., Verney V., Commereuc S., Fraïsse F. Self-reinforcement of polymers as a consequence of elongational flow. Rheol Acta 2006;45:366-373

10.   Song J., Prox M., Weber A., Ehrenstein G.W. Self-reinforcement of polypropylene. In: Polypropylene: Structure, Blends and Composites, Karger-Kocsis J. editors. London: Chapman and Hall, 1994. p. 271-291

11.   Prox M., Ehrenstein G. W. Polypropylene beim Spritzgießen eigenverstärken. Kunstst 1991;81:1057-1060

12.   Allan S. P., Bevis I. M., Zadhoush A. The development and application of shear controlled orientation technology. Iran J Polym. Sci Technol 1995;4:50-55

13.   Ogbonna C. I., Kalay G., Allan P. S., Bevis M. J. The self-reinforcement of polyolefins producted by shear controlled orientation in injection-molding. J Appl Polym Sci 1995;58:2131-2135

14. Lei J., Jiang C. D., Shen K. Z. Biaxially self-reinforced high-density polyethylene prepared by dynamic packing injection molding. I. Processing parameters and mechanical properties. J Appl Polym Sci 2004;93:1584-1590

15. Kalay G., Bevis M. J. Processing and physical property relationships in injection molded isotactic polypropylene. 1. Mechanical properties. J Polym Sci Pol Phys 1997;35:241-263

16. Guan Q., Shen K. Z., Ji L. L., Zhu J. M. Structure and properties of self-reinforced polyethylene prepared by oscillating packing injection-molding under low-pressure. J Appl Polym Sci 1995;55:1797-1804

17. Guan Q., Zhu X. G., Chiu D., Shen K. Z., Lai F. S., McCarthy S. P. Self-reinforcement of polypropylene by oscillating packing injection molding under low pressure. J Appl Polym Sci 1996;62:755-762

18. Chen L. M., Shen K. Z. Biaxial self-reinforcement of isotactic polypropylene prepared in uniaxial oscillating stress field by injection molding. I. Processing conditions and mechanical properties. J Appl Polym Sci 2000;78:1906-1910

19. Kalay G., Bevis M. J. Processing and physical property relationships in injection-molded isotactic polypropylene 2. Morphology and crystallinity. J Polym Sci Pol Phys 1997;35:265-291

20. Li Y. B., Chen J., Shen K. Z. Self-reinforced isotactic polypropylene prepared by melt vibration injection molding. Polym-Plast Technol 2008;47:673-677

21. Li Y. B., Shen K. Z. Effect of low-frequency melt vibration on HDPE morphology. Polym Int 2009;58:484-488

22. Naundorf I., Eyerer P. 'Living' or plastic hinges. In: Polypropylene an A-Z Reference, Karger Kocsis J. editors. Dordrecht: Kluwer Publishers, 1999. p. 383-391

23. Huang H. X. Mechanical anisotropy of self-reinforced polyethylene crystallized during continuous-melt extrusion. J Mater Sci Lett 1999;18:225-228

24. Ward I. M., Coates P. D., Dumoulin M. M. Solid Phase Processing of Polymers. Munich: Hanser, 2000.

25. Farrell C. J., Keller A. Direct ram extrusion of polyethylene; a correlation between chain-folding and tensile modulus. J Mater Sci 1977;12:966-974

26. Legros N., Ajji A., Dumoulin M. M. Ram extrusion of high-density polyethylene and polypropylene in solid state: Process conditions and properties. Polym Eng Sci 1997;37:1845-1852

27. Li J. X., Lee Y. W. Evolution of morpholgy in high-molecular-weight polyethylene during die drawing. J Mater Sci 1993;28:6496-6502

28. Taraiya A. K., Ward I. M. The production and properties of die-drawn biaxially oriented polypropylene tubes. Plast Rubber Compos Process Appl 1991;15:5-11

29. Mohanraj J., Chapleau N., Ajji A., Duckett R. A., Ward I. M. Production, properties and impact toughness of die-drawn toughened polypropylenes. Polym Eng Sci 2003;43:1317-1336

30. Taraiya A. K., Mirza M. S., Mohanraj J., Barton D. C., Ward I. M. Production and properties of highly oriented polyoxymethylene by die-drawing. J Appl Polym Sci 2003;88:1268-1278

31. Endo R., Kanamoto T. Superdrawing of polytetrafluoroethylene virgin powder above the static melting temperature. J. Polym. Sci. Pt. B-Polym. Phys. 2001;39:1995-2004

32. Bigg D. M., Smith E. G., Epstein M. M., Fiorentino R. J. High modulus semi-crystalline polymers by solid-state rolling. Polym Eng Sci 1982;22:27-33

33. Ajji A., Legros N. Solid-state forming of polypropylene. In: Polypropylene An A-Z Reference, J. K. K. editors. Dordrecht: Kluwer Publishers, 1999. p. 744-751

34. Morawiec J., Bartczak Z., Kazmierczak T., Galeski A. Rolling of polymeric materials with side constraints. Mater. Sci. Eng. A-Struct. Mater. Prop. Microstruct. Process. 2001;317:21-27

35. Bartczak Z. Deformation of high-density polyethylene produced by rolling with side constraints. I. Orientation behavior. J. Appl. Polym. Sci. 2002;86:1396-1404

36. Bartczak Z., Morawiec J., Galeski A. Deformation of high-density polyethylene produced by rolling with side constraints. II. Mechanical properties of oriented bars. J. Appl. Polym. Sci. 2002;86:1405-1412

37. Bartczak Z., Morawiec J., Galeski A. Structure and properties of isotactic polypropylene oriented by rolling with side constraints. J. Appl. Polym. Sci. 2002;86:1413-1425

38. Galeski A. Strength and toughness of crystalline polymer systems. Prog Polym Sci 2003;28:1643-1699

39. Mohanraj J., Morawiec J., Pawlak A., Barton D. C., Galeski A., Ward I. M. Orientation of polyoxymethylene by rolling with side constraints. Polymer 2008;49:303-316

40. Smith P., Lemstra P. J. Ultrahigh-Strength Polyetylene Filaments by Solution Spinning/Drawing. 2. Influence of Solvent on the Drawability. 1979;180:2983-2986

41. Barham P. J., Keller A. High-Strength Polyethylene Fibers From Solution and Gel Spinning. J. Mater. Sci. 1985;20:2281-2302

42. Pennings A. J., Vanderhooft R. J., Postema A. R., Hoogsteen W., Tenbrinke G. High-speed gel-spinning of ultra-high molecular weight polyethylene. Polym. Bull. 1986;16:167-174

43. Elyashevich G. K., Karpov E. A., Kudasheva O. V., Rosova E. Y. Structure and time-dependent mechanical behavior of highly oriented polyethylene. Mech Time-Depend Mat 1999;3:319-334

44. Elyashevich K. G., Karpov A. E., Rosova Y. E., Streltses V. B. Orientational crystallization and orientational drawing as strengthening methods for polyethylene. Polym Eng Sci 1993;33:1341-1351

45. Baranov A. O., Prut E. V. Ultra-high modulus isotactic polypropylene. 1. The influence of orientation drawing and initial morphology on the structure and properties of oriented samples. J Appl Polym Sci 1992;44:1557-1572

46. Morawiec J., Bartczak Z., Pluta M., Galeski A. High-strength uniaxially drawn tapes from scrap recycled poly(ethylene terephthalate). J. Appl. Polym. Sci. 2002;86:1426-1435

47. Marikhin V. A., Myasnikova L. P. Structural basis of high-strength high-modulus polymers. In: Oriented Polymer Materials, Fakirov S. editors. Heidelberg: Hüthing & Wepf Verlag Zug, 1996. p. 38-98

48. Alcock B., Cabrera N. O., Barkoula N. M., Peijs T. The effect of processing conditions on the mechanical properties and thermal stability of highly oriented PP tapes. Eur Polym J 2009;45:2878-2894

49. Karger-Kocsis J., Wanjale S. D., Abraham T., Bárány T., Apostolov A. A. Preparation and characterization of polypropylene homocomposites: Exploiting polymorphism of PP homopolymer. J Appl Polym Sci 2010;115:684-691

50. Ward I. M. Developments in oriented polymers, 1970-2004. Plast Rubber Compos 2004;33:189-194

51. Ward I. M., Hine P. J. The science and technology of hot compaction. Polymer 2004;45:1413-1427

52. Hine P. J., Ward I. M. High stiffness and high impact strength polymer composites by hot compaction of oriented fibers and tapes, in Mechanical Properties of Polymers based on Nanostructure and Morphology. In: Mechanical properties of polymers based on

nanostructure and morphology, Baltá-Calleja F. J.,Michler G. H. editors. Boca Raton: CRC Press, 2005. p. 677-698

53.   Rasburn J., Hine P. J., Ward I. M., Olley R. H., Bassett D. C., Kabeel M. A. The hot compaction of polyethylene terephthalate. J Mater Sci 1995;30:615-622

54.   Rojanapitayakorn P., Mather P. T., Goldberg A. J., Weiss R. A. Optically transparent self-reinforced poly(ethylene terephthalate) composites: molecular orientation and mechanical properties. Polymer 2005;46:761-773

55.   Hine P. J., Ward I. M., El Matty M. I. A., Olley R. H., Bassett D. C. The hot compaction of 2-dimensional woven melt spun high modulus polyethylene fibres. J Mater Sci 2000;35:5091-5099

56.   Hine P. J., Ward I. M., Jordan N. D., Olley R. H., Bassett D. C. A comparison of the hot-compaction behavior of oriented, high-modulus, polyethylene fibers and tapes. J Macromol Sci Phys 2001;B40:959-989

57.   Hine P. J., Ward I. M. Hot compaction of woven nylon 6,6 multifilaments. J Appl Polym Sci 2006;101:991-997

58.   Al Jebawi K., Sixou B., Seguela R., Vigier G., Chervin C. Hot compaction of polyoxymethylene, part 1: Processing and mechanical evaluation. J Appl Polym Sci 2006;102:1274-1284

59.   El-Maaty M. I. A., Bassett D. C., Olley R. H., Hine P. J., Ward I. M. The hot compaction of polypropylene fibres. J Mater Sci 1996;31:1157-1163

60.   Wright-Charlesworth D. D., Lautenschlager E. P., Gilbert J. L. Hot compaction of poly(methyl methacrylate) composites based on fiber shrinkage results. J Mater Sci-Mater Med 2005;16:967-975

61.   Ward I. M., Hine P. J. Novel composites by hot compaction of fibers. Polym Eng Sci 1997;37:1809-1814

62.   Ratner S., Weinberg A., Marom G. Neat UHMWPE filament wound composites by crosslinking compaction. Adv Compos Lett 2003;12:205-210

63.   Karger-Kocsis J. Interphase with lamellar interlocking and amorphous adherent - A model to explain effects of transcrystallinity. Adv Compos Lett 2000;9:225-227

64.   Ratner S., Pegoretti A., Migliaresi C., Weinberg A., Marom G. Relaxation processes and fatigue behavior of crosslinked UHMWPE fiber compacts. Compos Sci Technol 2005;65:87-94

65. Orench I. P., Balta-Calleja F., Hine P. J., Ward I. M. A microindentation study of polyethylene composites produced by hot compaction. J Appl Polym Sci 2006;100:1659-1663

66. Hine P. J., Ward I. M., Teckoe J. The hot compaction of woven polypropylene tapes. J Mater Sci 1998;33:2725-2733

67. Teckoe J., Olley R.H., Bassett D.C., Hine P.J., Ward I.M. The morphology of woven polypropylene tapes compacted at temperatures above and below optimum. 1999;34:2065-2073

68. Jordan N. D., Olley R. H., Bassett D. C., Hine P. J., Ward I. M. The development of morphology during hot compaction of Tensylon high-modulus polyethylene tapes and woven cloths. Polymer 2002;43:3397-3404

69. Hine P. J., Ward I. M., Jordan N. D., Olley R., Bassett D. C. The hot compaction behaviour of woven oriented polypropylene fibres and tapes. I. Mechanical properties. Polymer 2003;44:1117-1131

70. Jordan N. D., Bassett D. C., Olley R. H., Hine P. J., Ward I. M. The hot compaction behaviour of woven oriented polypropylene fibres and tapes. II. Morphology of cloths before and after compaction. Polymer 2003;44:1133-1143

71. Bozec L. Y., Kaang S., Hine P. J., Ward I. M. The thermal-expansion behaviour of hot compacted polypropylene and polyethylene composites. Compos Sci Technol 2000;60:333-344

72. Hine P. J., Olley R. H., Ward I. M. The use of interleaved films for optimising the production and properties of hot compacted, self reinforced polymer composites. Compos Sci Technol 2008;68:1413-1421

73. Hine P., Broome V., Ward I. The incorporation of carbon nanofibres to enhance the properties of self reinforced, single polymer composites. Polymer 2005;46:10936-10944

74. McKown S., Cantwell W. J. Investigation of strain-rate effects in self-reinforced polypropylene composites. J Compos Mater 2007;41:2457-2470

75. Prosser W., Hine P. J., Ward I. M. Investigation into thermoformability of hot compacted polypropylene sheet. Plast Rubber Compos 2000;29:401-410

76. Romhány G., Bárány T., Czigány T., Karger-Kocsis J. Fracture and failure behavior of fabric-reinforced all-poly(propylene) composite (Curv(R)). Polym Advan Technol 2007;18:90-96

77. Jenkins M. J., Hine P. J., Hay J. N., Ward I. M. Mechanical and acoustic frequency responses in flat hot-compacted polyethylene and polypropylene panels. J Appl Polym Sci 2006;99:2789-2796

78. Hine P. J., Astruc A., Ward I. M. Hot compaction of polyethylene naphthalate. J Appl Polym Sci 2004;93:796-802

79. Bárány T., Karger-Kocsis J., Czigány T. Development and characterization of self-reinforced poly(propylene) composites: carded mat reinforcement. Polym Advan Technol 2006;17:818-824

80. Bárány T., Izer A., Karger-Kocsis J. Impact resistance of all-polypropylene composites composed of alpha and beta modifications. Polym Test 2009;28:176-182

81. Izer A., Bárány T., Varga J. Development of woven fabric reinforced all-polypropylene composites with beta nucleated homo- and copolymer matrices. Compos Sci Technol 2009;69:2185-2192

82. Izer A., Bárány T. Hot consolidated all-PP composites from textile fabrics composed of isotactic PP filaments with different degrees of orientation. Express Polym Lett 2007;1:790-796

83. Varga J. Beta-modification of isotactic polypropylene: Preparation, structure, processing, properties, and application. J Macromol Sci Phys 2002;41:1121-1171

84. Varga J., Mudra I., Ehrenstein G. W. Highly active thermally stable beta-nucleating agents for isotactic polypropylene. J Appl Polym Sci 1999;74:2357-2368

85. Karger-Kocsis J. Composite composed of polypropylene reinforcement and polypropylene matrix and various production methods thereof. German Patent DE 102 37 803, 2007

86. Bárány T., Izer A., Czigány T. On consolidation of self-reinforced polypropylene composites. Plast Rubber Compos 2006;35:375-379

87. Varga J., Ehrenstein G. W., Schlarb A. K. Vibration welding of alpha and beta isotactic polypropylenes: Mechanical properties and structure. Express Polym Lett 2008;2:148-156

88. Abraham T. N., Siengchin S., Karger-Kocsis J. Dynamic mechanical thermal analysis of all-PP composites based on beta and alpha polymorphic forms. J Mater Sci 2008;43:3697-3703

89. Bhattacharyya D., Maitrot P., Fakirov S. Polyamide 6 single polymer composites. Express Polym Lett 2009;3:525-532

90. Chen J., Yang W., Yu G. P., Wang M., Ni H. Y., Shen K. Z. Continuous extrusion and tensile strength of self-reinforced HDPE/UHMWPE sheet. J Mater Process Tech 2008;202:165-169

91. Zhang G., Jiang L., Shen K. Z., Guan Q. Self-reinforcement of high-density polyethylene/low density polyethylene prepared by oscillating packing injection molding under low pressure. J Appl Polym Sci 1999;71:799-804

92. Zhang G., Fu Q., Shen K. Z., Jian L., Wang Y. Studies on blends of high-density polyethylene and polypropylene produced by oscillating shear stress field. J Appl Polym Sci 2002;86:58-63

93. Zhang A. Y., Jisheng E., Allan P. S., Bevis M. J. Enhancement in micro-fatigue resistance of UHMWPE and HDPE processed by SCORIM. J Mater Sci 2002;37:3189-3198

94. Capiati N. J., Porter R. S. Concept of one polymer composites modeled with high-density polyethylene. J Mater Sci 1975;10:1671-1677

95. Peijs T. Composites for recyclability. Mater Today 2003;6:30-35

96. Alcock B., Cabrera N. O., Barkoula N. M., Loos J., Peijs T. Interfacial properties of highly oriented coextruded polypropylene tapes for the creation of recyclable all-polypropylene composites. J Appl Polym Sci 2007;104:118-129

97. Cabrera N., Alcock B., Loos J., Peijs T. Processing of all-polypropylene composites for ultimate recyclability. Proc Inst Mech Eng Pt L-J Mater-Design Appl 2004;218:145-155

98. Alcock B., Cabrera N. O., Barkoula N. M., Loos J., Peijs T. The mechanical properties of unidirectional all-polypropylene composites. Compos Pt A-Appl Sci Manuf 2006;37:716-726

99. Alcock B., Cabrera N. O., Barkoula N. M., Peijs T. Low velocity impact performance of recyclable all-polypropylene composites. Compos Sci Technol 2006;66:1724-1737

100. Alcock B., Cabrera N. O., Barkoula N. M., Reynolds C. T., Govaert L. E., Peijs T. The effect of temperature and strain rate on the mechanical properties of highly oriented polypropylene tapes and all-polypropylene composites. Compos Sci Technol 2007;67:2061-2070

101. Alcock B., Cabrera N. O., Barkoula N. M., Spoelstra A. B., Loos J., Peijs T. The mechanical properties of woven tape all-polypropylene composites. Compos Part A-Appl Sci 2007;38:147-161

102. Alcock B., Cabrera N. O., Barkoula N. M., Wang Z., Peijs T. The effect of temperature and strain rate on the impact performance of recyclable all-polypropylene composites. Compos Part B-Eng 2008;39:537-547

103. Barkoula N. M., Alcock B., Cabrera N. O., Peijs T. Fatigue properties of highly oriented polypropylene tapes and all-polypropylene composites. Polym Polym Compos 2008;16:101-113

104. Karger Kocsis J. Fatigue performance of polypropylene and related composites. In: Polypropylene: An A-Z Reference, Karger-Kocsis J. editors. Dordrecht: Kluwer Publishers, 1999. p. 227-232

105. Banik K., Abraham T. N., Karger-Kocsis J. Flexural creep behavior of unidirectional and cross-ply all-poly(propylene) (PURE(R)) composites. Macromol Mater Eng 2007;292:1280-1288

106. Banik K., Karger-Kocsis J., Abraham T. Flexural creep of all-polypropylene composites: Model analysis. Polym Eng Sci 2008;48:941-948

107. Kim K. J., Yu W. R., Harrison P. Optimum consolidation of self-reinforced polypropylene composite and its time-dependent deformation behavior. Compos Part A-Appl S 2008;39:1597-1605

108. Cabrera N. O., Alcock B., Klompen E. T. J., Peijs T. Filament winding of co-extruded polypropylene tapes for fully recyclable all-polypropylene composite products. Appl Compos Mater 2008;15:27-45

109. Cabrera N., Reynold C. T., Alcock B., Peijs T. Non-isothermal stamp forming of continuous tape reinforced all-polypropylene composite sheet. Compos Part A-Appl S 2008;39:1455-1466

110. Alcock B., Cabrera N., Barkoula N., Peijs T. Direct forming of all-polypropylene composites products from fabrics made of co-extruded tapes. Appl Compos Mater 2009;16:117-134

111. Cabrera N. O., Alcock B., Peijs T. Design and manufacture of all-PP sandwich panels based on co-extruded polypropylene tapes. Compos Part B-Eng 2008;39:1183-1195

112. Shalom S., Harel H., Marom G. Fatigue behaviour of flat filament-wound polyethylene composites. Compos Sci Technol 1997;57:1423-1427

113. Houshyar S., Shanks R. A. Morphology, thermal and mechanical properties of poly(propylene) fibre-matrix composites. Macromol Mater Eng 2003;288:599-606

114. Houshyar S., Shanks R. A. Tensile properties and creep response of polypropylene fibre composites with variation of fibre diameter. Polym Int 2004;53:1752-1759

115. Houshyar S., Shanks R. A., Hodzic A. Tensile creep behaviour of polypropylene fibre reinforced polypropylene composites. Polym Test 2005;24:257-264

116. Houshyar S., Shanks R. A., Hodzic A. Influence of different woven geometry in poly(propylene) woven composites. Macromol Mater Eng 2005;290:45-52

117. Houshyar S., Shanks R. A. Mechanical and thermal properties of flexible poly(propylene) composites. Macromol Mater Eng 2006;291:59-67

118. Houshyar S., Shanks R. A. Mechanical and thermal properties of toughened polypropylene composites. J Appl Polym Sci 2007;105:390-397

119. Houshyar S., Shanks R. A., Hodzic A. Modelling of polypropylene fibre-matrix composites using finite element analysis. Express Polym Lett 2009;3:2-12

120. Bárány T., Izer A., Czigány T. High performance self-reinforced polypropylene composites. Mater Sci Forum 2007;567-538:121-128

121. Izer A., Bárány T. Effect of consolidation on the flexural creep behaviour of all-polypropylene composite. Express Polym Lett 2010;4:210-216

122. Kitayama T., Utsumi S., Hamada H., Nishino T., Kikutani T., Ito H. Interfacial properties of PP/PP composites. J Appl Polym Sci 2003;88:2875-2883

123. Wu C. M., Chen M., Karger-Kocsis J. Interfacial shear strength and failure modes in sPP/CF and iPP/CF microcomposites by fragmentation. Polymer 2001;42:129-135

124. Bárány T., Izer A., Menyhard A. Reprocessability and melting behaviour of self-reinforced composites based on PP homo and copolymers. J Therm Anal Calorim in press

125. Ruan W. H., Zhang M. Q., Wang M. H., Rong M. Z., Bárány T., Czigány T. Preparation and properties of nano-silica filled self-reinforced polypropylene. Adv Mater Res 2008;47:318-321

126. Pegoretti A. Z. A., Migliaresi C. Preparation and tensile mechanical properties of unidirectional liquid crystalline single-polymer composites. Compos Sci Technol 2006;66:1970-1979

127. Pegoretti A., Zanolli A., Migliaresi C. Flexural and interlaminar mechanical properties of unidirectional liquid crystalline single-polymer composites. Compos Sci Technol 2006;66:1953-1962

128. Pegoretti A. Trends in composite materials: the challenge of single-polymer composites. Express Polym Lett 2007;1:710-710

129. Fakirov S., Evstatiev M., Friedrich K. From Polymer Blends to Microfibrillar reinforced Composites. In: Polymer Blends, Volume 2: Performance, Paul D. R.,Bucknall C. B. editors. New York: Wiley-Interscience Publication, 2000. p. 455-475

130. Boulahia R., Gloaguen J. M., Zadri F., Nadt-Abdelaziz M., Seguela R., Boukharouba T., Lefebvre J. M. Deformation behaviour and mechanical properties of polypropylene processed by equal channel angular extrusion: Effects of back-pressure and extrusion velocity. Polymer 2009;50:5508-5517

Figure captions

Fig. 1.　　　Classification of self-reinforced polymeric materials (SRPMs), *not yet explored

Fig. 2.　　　Scheme of the 1D supermolecular structure formation in a die with a convergent section during extrusion molding

Fig. 3.　　　Scheme of the function of the SCORIM procedure along with the three basic operations (A, B and C) –Mode A: the pistons are activated 180° out of phase; Mode B: pistons are activated in phase; the pistons are held down a constant pressure

Fig. 4.　　　Working principle of the vibration injection molding

Fig. 5.　　　Working principle of the hydrostatic extrusion process schematically

Fig. 6.　　　Working principle of the die-drawing a: unoriented phase, b: oriented phase

Fig. 7.　　　Scheme of chain orientation

Fig. 8.　　　Principle sketch of hot compaction on the example of unidirectional (UD) arranged fibers

Fig. 9.　　　Longitudinal flexural modulus (●) and transverse strength (■) vs. compaction temperature of melt spun polyethylene fibers

Fig. 10.　　　Effects of testing temperature on the stress-strain behavior of self-reinforced PP with 2D reinforcement, schematically. (a) Dependence of yield strain (●) and failure strain (■) as a function of temperature; (b) dependence of yield stress (●) and failure stress (■) as a function of temperature

Fig. 11.　　　Scheme of the composite processing via film stacking

Fig. 12.　　　Transcrystalline layer of PP fiber and β-rPP matrix

Fig. 13.　　　Schematic representation of the self-reinforcing sheet extrusion die: (1) temperature controlling oil bath, (2) the straight section, (3), the convergent section, and (4) double functional temperature–pressure sensor

Fig. 14.　　　Coextrusion technology with additional stretching to produce high-strength tapes

Fig. 15.　　　Production of composites with UD tape alignment from coextruded tapes

Fig. 16.　　　Lamellar structure within the transcrystalline layer as a function of the consolidation temperature

Fig. 17.   Hypothesized interphase with lamellar interlocking and amorphous phase as adherent for the transcrystaline layer initiated by flat-on type lamellar growth on fiber surface

Tables

Table 1   Production method, conditions and product characteristics of single-component SRPMs produced in one-step (in situ)

Table 2   Possible polymer pairs to produce SRPMs; * single component SRPM; × production occurs via liquid composite molding.

Table 3   Production method, conditions and product characteristics of single-component SRPMs produced in multi-step (ex situ) (*summarized results)

Table 4   Production method, conditions and product characteristics of multi-component SRPMs produced in single-step (in situ)

Table 5   Production method, conditions and product characteristics of multi-component SRPMs produced in multi-step (ex situ)